Applied Energy 289 (2021) 116713

Contents lists available at ScienceDirect

Applied Energy

journal homepage: www.elsevier.com/locate/apenergy

Integrated electricity, hydrogen and methane system modelling framework: Application to the Dutch Infrastructure Outlook 2050

Binod Koirala [a,*], Sebastiaan Hers [a], Germán Morales-España [a], Özge Özdemir [b], Jos Sijm [a], Marcel Weeda [a]

[a] TNO Energy Transition, Radarweg 60, 1043 NT Amsterdam, the Netherlands
[b] PBL Netherlands Environmental Assessment Agency, Bezuidenhoutseweg 30, 2594 AV The Hague, the Netherlands

HIGHLIGHTS

- Electricity, hydrogen and methane system will be more integrated in the future.
- The developed integrated model considers their interactions and interdependencies.
- As proof-of-concept, the model is applied to the Dutch Infrastructure Outlook 2050.
- Interweaving electricity, hydrogen and methane system will provide much needed flexibility.

ARTICLE INFO

Keywords:
Energy system integration
Sector-coupling
Methane
Hydrogen
Flexibility
Energy transition
Energy markets

ABSTRACT

The future energy system is widely expected to show increasing levels of integration across differing energy carriers. Electricity, hydrogen, methane and heat systems may become increasingly interdependent due to coupling through conversion and hybrid energy technologies. Market parties, network operators, policy makers and regulators require tools to capture implications of possible techno-economic and institutional developments in one system for the operation of others. In this article, we provide an integrated electricity, hydrogen and methane systems modelling framework focusing on interdependencies between them. The proposed integrated electricity and (renewable) gas system model is a market equilibrium model with hourly price and volume interactions, considering ramp rates of conventional units, variability of intermittent renewables, conversion, transport as well as storage of electricity, hydrogen and methane. The integrated model is formulated as a linear program under the assumption of perfect competition. As proof-of-concept, the model has been applied to a test case consisting of 34 electricity nodes, 19 hydrogen nodes and 22 methane nodes, reflecting the regional governance scenario in the Dutch Infrastructure Outlook 2050 study. The case study also includes different sensitivity analyses with regard to variable renewable capacity, energy demand and biomass prices to illustrate model response to perturbations of its main drivers. This article demonstrates that the interweaving of electricity, hydrogen and methane systems can provide the required flexibility in the future energy system.

Nomenclature

The parameters and sets are denoted upper-case letters whereas variables, functions and indexes are represented by lower-case letters.

Sets and indexes	
$i, i' \in I$	set of nodes for hydrogen, methane and electricity network
$J(i) \in I$	set of nodes connected to node i through an electric line

(*continued on next column*)

(*continued*)

Sets and indexes	
$JHG(i) \in I$	set of nodes connected to node i through a hydrogen pipeline
$JHL(i) \in I$	set of nodes connected to node i through liquified hydrogen shipment
$JMG(i) \in I$	set of nodes connected to node i through a gas pipeline
$JML(i) \in I$	set of nodes connected to node i through liquefied gas shipment
$p \in P$	set of period (hours)
$f \in F$	set of hydrogen storage types

(*continued on next page*)

* Corresponding author.
E-mail address: binod.koirala@tno.nl (B. Koirala).

https://doi.org/10.1016/j.apenergy.2021.116713
Received 9 October 2020; Received in revised form 18 February 2021; Accepted 19 February 2021
Available online 4 March 2021

(*continued*)

Sets and indexes	
$r \in R$	set of electrical storage types
$n \in N$	set of methane storage types
$h \in H$	set of power plants
$nfp \in NFP \subset H$	set of natural gas fired power units
$hfp \in HFP \subset H$	set of hydrogen fired power units
$gfp \in GFP \subset H$	set of green gas fired power units
$vre \in VRE \subset H$	set of all variable renewables units
$oth \in OTH \subset H$	set of all remaining power generation units
Variables and parameters electricity system	
q^{e}_{ihp}	electricity generation by unit h at node i in period p [MWh]
$q^{e}_{i(hfp)p}$	electricity generation by hydrogen fired units *hfp* at node i in period p [MWh]
$q^{e}_{i(nfp)p}$	electricity generation by natural gas fired units *nfp* at node i in period p [MWh]
$q^{e}_{i(gfp)p}$	electricity generation by green gas fired units *gfp* at node i in period p [MWh]
ds^{e}_{irp}	electricity discharge at node i of storage type r in period p [MWh]
ch^{e}_{irp}	electricity charging at node i of storage type r in period p [MWh]
sol^{e}_{irp}	Energy storage level at node i of storage type r in period p [MWh]
$flow^{e}_{ii'p}$	electricity flow from node i to node i' in period p [MWh]
ens^{e}_{ip}	electricity demand not served at node i in period p [MWh]
D^{e}_{ip}	electricity demand at node i in period p [MWh]
$d^{eH_2}_{ip}$	electricity demand for electrolysis at node i in period p [MWh]
$price^{e}_{ip}$	dual variable reflecting electricity prices at node i in period p [€/MWh]
c^{e}_{ihp}	marginal costs of unit h at node i in period p [€/MWh]
cr^{e}_{irp}	marginal cost of electrical storage type r at node i in period p [€]
$VOLL^{e}$	value of lost load for electricity system [€/MWh]
$PCO2$	cost of CO_2 emissions [€/tonne]
Θ^{e}_{h}	emission factor of unit h [tonne/MWh]
$T^{e}_{ii'}$	import/export transmission capacity between node i and i' [MW]
AF^{e}_{ih}	availability factor of unit h in node i
CF^{e}_{ihp}	capacity factor of variable renewables unit h in node i in period p
OM^{e}_{ih}	operation and maintenance cost of unit h in node i [€/MWh]
η^{e}_{ih}	electrical efficiency of unit h in node i [p.u.]
Q^{e}_{hi}	capacity of unit h in node i [MW]
RR^{e}_{ih}	maximum ramp rate of unit h in node i [MW/hour]
PS^{e}_{ir}	electrical pumping/turbine capacity at node i *of* storage type r [MWh/hour]
SC^{e}_{irp}	electrical storage capacity at node i *of* storage type r [MWh]
ISC^{e}_{r0}	initial energy level *of* storage type r at node i *at hour 0* [MWh]
EFF^{r}	efficiency of electrical storage facility depending on the storage type r [p.u.]
Variables and parameters hydrogen system	
$q^{bgH_2}_{ip}$	hydrogen generation (biomass gasification) at node i in period p [MWh]
$q^{gH_2}_{ip}$	hydrogen generation (natural gas reforming) at node i in period p [MWh]
$q^{eH_2}_{ip}$	hydrogen generation (electrolysis) at node i in period p [MWh]
$tl^{H_2}_{ii'p}$	liquid hydrogen transport from i to i' in period p [MWh]
$flow^{H_2}_{ii'p}$	pipeline hydrogen flow from i to i' in period p [MWh]
x^{in}_{ip}	regasified hydrogen at node i in period p [MWh]
x^{out}_{ip}	liquified hydrogen at node i in period p [MWh]
ens^{H2}_{ip}	hydrogen demand not served at node i in period p [MWh]
$e^{H_2}_{ifp}$	Hydrogen extracted from storage type f at node i in period p [MWh]
$inj^{H_2}_{ifp}$	hydrogen injected into storage type f at node i in period p [MWh]
$D^{H_2}_{ip}$	residential and industrial hydrogen demand in node i in period p [MWh]
$d^{H_2e}_{ip}$	hydrogen demand for power generation at node i in period p [MWh]
$price^{H2}_{ip}$	dual variable reflecting hydrogen prices at node i in period p [€/MWh]
$VOLL^{H2}$	value of lost load for hydrogen system [€/MWh]
η^{eH2}_{i}	efficiency of electrolysis unit in node i [p.u.]
c^{bgH2}_{ip}	hydrogen production cost (biomass gasification) at node i in period p [€/MWh]
c^{gH2}_{ip}	hydrogen production cost (NG reforming) at node i in period p [€/MWh]
c^{eH2}_{ip}	hydrogen production cost (electrolysis) at node i in period p [€/MWh]
$CS^{H_2}_{i}$	operational cost of storage type f in node i [€/MWh]

(*continued on next column*)

(*continued*)

Sets and indexes	
$CX^{H_2}_{ii'}$	cost of transporting liquid hydrogen between node i *and* i' [€/MWh]
$CZ^{H_2}_{ii'}$	cost of transporting hydrogen via pipeline between node i *and* i' [€/MWh]
$CL^{H_2}_{i}$	hydrogen liquefaction cost at node i [€/MWh]
$CG^{H_2}_{i}$	hydrogen gasification cost at node i [€/MWh]
$Q^{gH_2}_{i}$	hydrogen production capacity (natural gas reforming) at node i *[MW]*
$Q^{bgH_2}_{i}$	hydrogen production capacity (biomass gasification) at node i *[MW]*
$Q^{eH_2}_{i}$	hydrogen production capacity (electrolysis) at node i [MW]
$SC^{H_2}_{if}$	annual working hydrogen capacity of storage type f at node i [MWh]
$SER^{H_2}_{if}$	extraction rate of storage type f at node i [MWh/hour]
$SIR^{H_2}_{if}$	injection rate of storage type f at node i [kcm/hour]
$TG^{H_2}_{ii'}$	capacity of hydrogen pipeline ii' [MW]
TLG^{out}_{i}	hydrogen liquefaction capacity at node i [MW]
TLG^{in}_{i}	hydrogen regasification capacity at node i [MW]
Θ^{gH2}	emission factor of natural gas to hydrogen conversion [tonne/MWh]
$\eta^{gH_2}_{i}$	efficiency of natural gas to hydrogen conversion in node i
OM^{gH2}_{i}	O&M cost of gas to hydrogen conversion at node i [€/MWh]
OM^{eH2}_{i}	O&M cost of electrolysis at node i [€/MWh]
Variables and parameters methane system	
q^{ng}_{zip}	methane (natural gas) production at unit z in node i in period p [MWh]
q^{gg}_{ip}	methane (green gas) production at node i in period p [MWh]
q^{H2g}_{ip}	methane production from hydrogen at node i in period p [MWh]
$flow^{g}_{ii'p}$	methane transport via pipeline from i to i' in period p [MWh]
$tl^{g}_{ii'p}$	liquified methane shipping from i to i' in period p [MWh]
x^{gin}_{ip}	regasified methane at node i in period p [MWh]
x^{gout}_{ip}	liquified methane at node i in period p [MWh]
e^{g}_{inp}	methane extracted from storage type n at node i in period p [MWh]
inj^{g}_{inp}	methane injected into storage type n at node i in period p [MWh]
ens^{g}_{ip}	methane demand not served at node i in period p [MWh]
d^{ge}_{ip}	methane demand for electricity generation at node i in period p [MWh]
D^{g}_{ip}	residential and industrial methane demand at node i in period p [MWh]
d^{gH2}_{ip}	natural gas demand for hydrogen production at node i in period p [MWh]
$price^{g}_{ip}$	dual variable reflecting methane prices at node i in period p [€/MWh]
$VOLL^{g}$	value of lost load for methane system [€/MWh]
c^{ng}_{zi}	natural gas production cost at unit z in node i [€/MWh]
c^{gg}_{i}	green gas (methane) production cost at node i [€/MWh]
c^{H2g}_{i}	methanation cost at node i [€/MWh]
CS^{g}_{i}	operational cost of storage in node i [€/MWh]
$CX^{g}_{ii'}$	cost of transporting liquid methane between node i *and* i' [€/MWh]
$CZ^{g}_{ii'}$	cost of methane pipeline transport between node i *and* i' [€/MWh]
CL^{g}_{i}	methane liquefaction cost at node i [€/MWh]
CG^{g}_{i}	methane gasification cost at node i [€/MWh]
Q^{g}_{zi}	natural gas production capacity of unit z at node i [MW]
Q^{gg}_{i}	green gas (methane) production capacity at node i [MW]
Q^{H2g}_{i}	methanation capacity at node i [MW]
$\eta^{H_2g}_{i}$	efficiency of methanation at node i
SC^{g}_{in}	annual working gas capacity of methane storage type n at node i [MWh]
SER^{g}_{in}	methane extraction rate of storage type n at node i [MW/hour]
SIR^{g}_{in}	methane injection rate of storage type n at node i [MW/hour]
$TG^{g}_{ii'}$	capacity of methane pipeline between node i *and* i' [MW]
$TLNG^{out}_{i}$	methane liquefaction capacity at node i [MW]
$TLNG^{in}_{i}$	methane regasification capacity at node i [MW]

1. Introduction

To meet renewable energy and emission targets, several countries around the world are adopting ambitious decarbonization strategies such as increased utilization of renewables for power generation [1], sector coupling [2] as well as electrification of different sectors [1–3]. The energy transition towards more sustainable and low carbon energy

systems implies 1) a larger share of electricity from renewable energy resources such as wind and solar with increased variability and uncertainty [1], 2) a larger share of electricity in total energy use due to the increasing penetration of flexible demand technologies such as electric vehicles (EVs) [3–5], heat pumps (HPs) [6,7], power-to-gas (P2G) [8,9], 3) a larger share of renewable gas such as hydrogen and green gases [8,9], and 4) a higher need for system integration and flexibility to cover substantially higher variations in renewable electricity generation and demand [10]. To accelerate the energy transition, it is then paramount to increase the level of integration between different energy carriers such as electricity, heat, methane and hydrogen not only in terms of markets but also in terms of infrastructures [2].

Variable renewable resources, like wind and solar, offer a vast potential for energy system decarbonisation. Yet, large-scale rollout of wind and solar faces a major challenge in market and system integration. Electrification of energy demand sectors and enhancing demand flexibility may offer one solution pathway for these flexibility challenges [10,11]. Hybrid energy systems that allow to serve non-electrifiable energy and feedstock demand with conversion of renewable electricity production is expected to offer another cost-effective solution pathway [12]. Here, renewable electricity may be used to produce renewable gases like hydrogen, and synthetic gases. This paradigm shift beyond electrification is, for example, well captured by the vision of the Dutch electricity transmission system operator TenneT and gas transmission system operator Gasunie, as clearly reflected in their Infrastructure Outlook (IO2050) report published in 2019, where they present an integrated power and (renewable) gas system outlook as a pathway to system decarbonization for both electrons and molecules [13].

Interest in modelling different forms of integrated energy systems has been growing over time in order to address the challenges of the energy transition towards a carbon–neutral energy system. Analysing the drivers, requirements and opportunities of integrated multi-energy systems, Mancarella et al. (2016) highlight the need for closer attention to all energy vectors and infrastructures that supply the end-use demand [14]. Riepin et al. (2018) develop an integrated investment model for electricity and gas markets and find out that the uncertainty in gas demand leads to an overall decrease of investments in gas-fired power plants [15]. Özdemir et al. (2015) conclude that the availability of flexible gas supply such as peak gas storage in the gas market determine the competitiveness and future role of gas-fired power plants in the power market [16]. Ordoudis, Pinson and Morales (2019) find out that the coupled operation of electricity and natural gas systems facilitates renewable energy integration [17]. Abeysekera, Wu and Nick (2016) highlight the need to develop robust methods and tools for modelling analysis of integrated energy sytems [18]. Pambour et al. (2018) reveal that to capture bi-directional interdependencies between gas and electricity networks requires the use of combined simulation models [19]. Juanwei et al. (2019) put forward the need to extend reliability assessment to integrated energy systems coupling with other kinds of energies [20]. Tsupari, Karki and Vakkilainen (2016) reveal that the integration of power-to-gas with biomass-fired combined heat and power plant offers an economically feasible concept for future energy system [21]. Farahani et al. (2020) study hydrogen-based integrated energy and mobility system and find out that using hydrogen storage is much cheaper than using large battery storage system [22]. As further elaborated in Section 2, several of these studies either consider interactions between gas and electricity markets without considering the hydrogen system or they include hydrogen in their analysis but lack interactions with other energy systems and infrastructures. None of these studies, to our knowledge, captures the interactions and dynamics of integrated electricity, methane, and hydrogen systems & markets, including interdependencies through conversion and hybrid energy technologies set-ups as well as the energy transport infrastructure in these markets. In this article, we fill this gap by proposing a modelling framework to adequately analyse the challenges and opportunities for the electricity and (renewable) gas systems and markets, including the interlinkages between these markets. This article presents an optimization model for the operation of integrated electricity, hydrogen and methane value chains. The proposed integrated electricity and (renewable) gas market model provides the least-cost simultaneous hourly dispatch of power, hydrogen and methane, while taking into account the interlinkages between them. The integrated model presented in this article is valuable for the decision support as well as efficient operation and co-ordination among electricity, hydrogen and methane value chains. The model can be used to assess future interactions between electricity and gas markets and may be the basis for future energy system analysis on investments in conversion, transport, storage and system decarbonization.

The rest of the article is organized as follows. Section 2 presents the research framework for the integrated electricity and (renewable) gas model (I-ELGAS), followed by model formulation in Section 3. Section 4 describes the future energy system in the Netherlands and introduces the case study based on the regional scenario of the IO2050 study. In Section 5, results from the IO2050 baseline scenario and some sensitivity analyses are presented and explained briefly, followed by a conclusion and discussion of the main findings and limitations of the current paper in Section 6 and Section 7.

2. Research framework

Traditionally, electricity, methane and hydrogen systems are planned and operated independently. However, increasing interactions and interdependencies between electricity, methane and hydrogen systems (see Fig. 1) may offer a cost-effective pathway to absorb large volumes of variable renewable energy in the energy system. Water electrolysis plants interlink electricity and hydrogen systems as electricity is used to produce hydrogen. Several technologies for electrolysis such as alkaline [23], polymer electrolyte membrane (PEM) and solid-oxide electrolysers [24–26] are available [8,27–29]. Natural gas reformers, such as steam methane reforming (SMR) [30] and auto-thermal reforming (ATR) [31,32], interlink methane and hydrogen systems as natural gas is used to produce grey or blue hydrogen (i.e. with carbon capture and storage (CCS)). At the same time, synthetic methane can be produced via hydrogen by catalytic [33] or biological [34] methanation processes [29,35]. Hydrogen-fired power plants interlink hydrogen and electricity systems [36,37]. Methane-fired combined heat and power generation (CHP) [21,38], open cycle gas turbines (OCGT) [39], and combined cycle gas turbines (CCGT) [40] link electricity and methane systems. Electricity storage in the form of batteries [41–43], including electric vehicles, as well as underground hydrogen [44–46] and methane storage [47] help to decouple the instantaneous mismatch between supply and demand [43,48]. With increasing renewables in the power system and

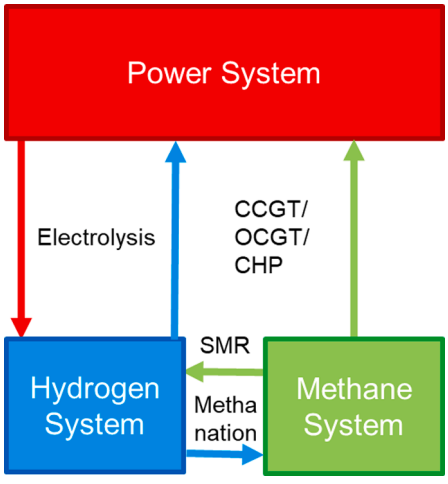

Fig. 1. Interdependencies between electricity, hydrogen and methane systems.

associated system needs for flexibility, the interactions between these markets and systems are commonly expected to increase in the future.

There is a growing body of literature on the analysis of different aspects of sector coupling or cross-sector integration. Reichmann et al. (2019) define sector coupling as linking both markets and infrastructures of the electricity and gas sectors [2]. Based on a spatially and temporally resolved open source energy model for cross-sector and cross-border integration of renewables, Brown et al. (2018) show that tighter sector coupling through power-to-gas and thermal energy storage reduces the need of grid re-enforcements [49]. Robinious et al. (2017) perform an extensive review of available research as well as modelling on linking the power and transport sectors [3,50]. Maruf (2019) provides a review on different energy system modelling perspectives for sector coupling in the North Sea region [51].

A large volume of literature also includes hydrogen production and deployment in their analysis. Buttler and Spliethoff (2018) review the potential of water electrolysis in coupling electricity, heating, mobility and chemical industry sector [8]. Eriksson and Gray (2017) review approaches for integrating hydrogen energy technologies into hybrid energy systems [52]. Yan et al. (2018) conduct cost-benefit analysis of avoiding renewables curtailment by converting and transporting it as hydrogen [53]. Using JRC-EU-TIMES model, Blanco et al. (2018) study the role of hydrogen-based power-to-liquid in achieving 80–95% decarbonization by 2050 [48]. Uyar and Bezikci (2017) analyse the role of hydrogen in 100% renewable energy systems [54]. Lecker et al. (2017) perform a review of biological hydrogen methanation approaches [34]. Kaiwen et al. (2018) as well as Mondal and Ramesh Chandran (2014) conduct a comprehensive study on economic and environmental aspects of hydrogen production using steam methane reforming [30,55]. Glenk and Reichelstein (2019) suggest that renewable hydrogen is already cost-competitive in niche applications [56]. Michalski et al. (2017) reveal that optimization of electrolysis-based hydrogen production and hydrogen storage in salt-caverns will have a positive impact on the power system due to reduced curtailments as well as residual peaks [45]. Welder et al. (2018) developa methodology to determine cost-optimal design and operation of future energy systems with power to hydrogen scenarios in Germany [57]. Qadrdan et al. (2015) investigate the role of power-to-gas (hydrogen) on gas and electricity network considering different allowable levels of hydrogen injection [58]. However, these articles lack comprehensive interactions between other markets and infrastructures. This article fills this gap by taking into account the interactions and interdependencies between electricity, hydrogen and methane systems and markets.

Several studies consider integral modelling of interactions between gas and electricity markets. Qadrdan et al. (2010) analyse the impact of large-scale wind generation on the gas network of Great Britain using a combined gas and electricity network model [59]. Abrell et al. (2013) claim that interdependence of electricity and natural gas is becoming a major energy policy as well as regulatory issue and analyse the impact of natural gas network on electricity market until 2050 in Europe [60]. Blanco et al. (2018) conclude that system drivers such as CO_2 storage potential and variable renewable penetration level exert more influence over power to methane potential than the technology drivers [61]. Guilera et al. (2018) analyse the economic viability of synthetic natural gas production from power and CO_2, and claim that it has potential for continuous and seasonal production in the future [62]. Ghaib and Ben-Fares (2018) provide a comprehensive review on power to methane conversion including intermediate steps such as electrolysis and methanation [63]. Mi and Khodayar (2019) show that the coordinated operation of the electricity and natural gas networks considering the line pack flexibility in the natural gas pipelines lead to lower operation costs [64]. Co-simulating an interconnected power and natural gas system, Craig et al. (2020) conclude that co-ordination between power and gas systems reduces power system cost and increases gas deliverability [65]. Juanwei et al. (2019) perform reliability assessment of integrated electricity and gas system considering different dispatch strategies [20]. Özdemir et al. (2015) propose an integrated electricity and natural gas market modelling framework focusing on short term interdependencies that relate to price and volume interactions between electricity and natural gas markets [16]. Chaudry et al. (2014) develop a combined gas and electricity network expansion planning model considering gas-fired power plants as linkages between the two networks [66]. Using a combined gas and electricity network expansion model, Qadrdan et al. (2017) analyse the impact of demand-side response on the electricity and gas supply system in Great Britain [67]. Ameli et al. (2020) demonstrate that the deployment of flexibility technologies supports the interaction between gas and electricity system [68]. However, none of these approaches considers the hydrogen system. Moreover, the interdependencies between different markets and infrastructures are rarely or only marginally considered with limited geographical and temporal scope. Hence, our model improves on these approaches by combining hydrogen, electricity, and natural gas systems and markets.

In addition, several studies such as the *Infrastructure Outlook 2050* and *Grid for the Future*, present an integrated power and (renewable) gas system outlook as an important requirement to system decarbonization for both electrons and molecules [13,69]. Yet, analysis of future interactions between energy supply and demand requires a market-based system allocation model that accounts for interactions between these markets and simultaneously represents the infrastructures in these markets. Such an integrated model, as presented in Section 3, may provide the basis for future energy system analysis on investments in conversion, transport, storage and system decarbonization.

3. Mathematical formulation

Modelling the interaction between electricity, gas and hydrogen systems results in a large-scale model. For real-life systems, model size increases exponentially with the geographical and temporal scope. Using LP reduces computational times significantly and allows us to address large-scale problems. For electricity and gas systems, linearization of flows and processes and using LP models are common practice in the literature [70–75]. Modelling the problem as an LP may sacrifice some model capabilities (discussed in Section 6), but this choice allows the model to be able to solve the ambitious spatial (different nodes for different networks) and temporal granularity (8760 h) that were defined within their main aims. This high temporal granularity also allows us to precisely model the (seasonal) storage within a full year, this accuracy is usually sacrificed in models with lower temporal granularity for the sake of computational tractability [76].

The Özdemir et al. (2015) framework of the integrated power and natural gas market model provides the basis for this integrated power and (renewable) gas market model [16]. In the proposed integrated model (I-ELGAS), the hydrogen system is added and the methane system is expanded to include natural gas as well as bio-based and synthetic gas. The electricity system is also expanded to include hydrogen and methane-fired power generation. In addition, the temporal granularity has been improved from one week per season to hourly simulation of a year. The geographical scope has also been improved from one node per country to multiple nodes to resemble with the existing and foreseen transport infrastructures of the electricity, hydrogen and methane systems. Fig. 2 illustrates the schematic of the proposed integrated model of electricity, hydrogen and methane systems. Here we present a linear program (LP) model which objective is to minimize the total operational costs of the integrated electricity, hydrogen and gas systems. The I-ELGAS model covers nine North Sea countries providing hourly simulations for a full year. In this study however, the I-ELGAS model is applied only to one of the four scenarios developed for the Netherlands and Germany in the IO2050 study [13]. In addition the application presented in this paper is limited to the Dutch subsystem in this scenario as only the Dutch scenario data were made available by the authors of IO2050. The main outputs are hourly (nodal) energy prices for electricity, hydrogen and methane (i.e., commodity prices assuming perfect

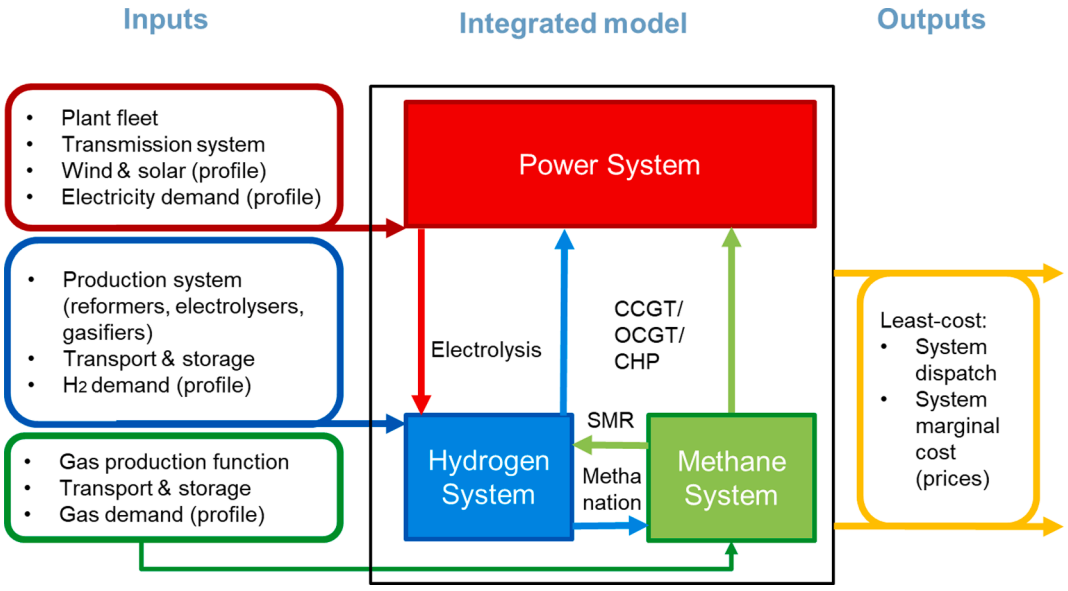

Fig. 2. Integrated electricity, hydrogen and gas market model (I-ELGAS) schematic.

competition), energy balances as well as optimal dispatch of each subsystem. The I-ELGAS model is implemented in AIMMS [77] and the LP problem solved using CPLEX 12.9 [78]. The energy flows are geographically visualized using the mapeditor based on open-source energy system description language (ESDL) [79].

The integrated model is formulated as an equivalent single optimization problem assuming perfectly competitive markets. The objective function is to minimize the total operational costs of the system satisfying generation, transmission and storage constraints:

$$\min\left[cost^{elec} + cost^{H2} + cost^{g}\right] \tag{1}$$

where,

$$cost^{elec} = \sum_{i\in I, p\in P}\left[\sum_{h\in H} c^{e}_{ihp}.q^{e}_{ihp} + \sum_{r\in R} cr^{e}_{irp}.ch^{e}_{irp} + VOLL^{e}.ens^{e}_{ip}\right] \tag{2}$$

$$cost^{H2} = \sum_{i\in I, p\in P}\left[\begin{array}{c} c^{bgH2}_{ip}.q^{bgH_2}_{ip} + c^{gH2}_{ip}.q^{gH_2}_{ip} + c^{eH2}_{ip}.q^{eH_2}_{ip} + CL^{H_2}_{i}.x^{out}_{ip} + CG^{H2}_{i}.x^{in}_{ip} + \\ \sum_{i'\in JHG(i)} CZ^{H2}_{ii'}.flow^{H2}_{ii'p} + \sum_{i'\in JHL(i)} CX^{H2}_{ii'}.tl^{H2}_{ii'p} + \sum_{f\in F} CS^{H2}_{i}.inj^{H2}_{ifp} + VOLL^{H2}.ens^{H2}_{ip} \end{array}\right] \tag{3}$$

$$cost^{g} = \sum_{i\in I, p\in P}\left[\begin{array}{c} \sum_{z\in Z} c^{ng}_{zi}.q^{ng}_{zip} + c^{gg}_{i}.q^{gg}_{ip} + c^{H2g}_{i}.q^{H2g}_{ip} + CL^{g}_{i}.x^{gout}_{ip} + CG^{g}_{i}.x^{gin}_{ip} + \\ \sum_{i'\in JMG(i)} CZ^{g}_{ii'}.flow^{g}_{ii'p} + \sum_{i'\in JML(i)} CX^{g}_{ii'}.tl^{g}_{ii'p} + \sum_{n\in N} CS^{g}_{i}.inj^{g}_{inp} + VOLL^{g}.ens^{g}_{ip} \end{array}\right] \tag{4}$$

For variable renewable generation units, the electricity production cost (c^{e}_{ihp}) depends only on operation and maintenance costs. The production cost in (1) for hydrogen-fired units and green gas fired units (c^{e}_{ihp}) depends also only on operation and maintenance costs, as their associated hydrogen and methane costs are endogenous. The production costs of the conventional units depend on fuel prices (FP^{e}_{ihp}), emission factors (Θ^{e}_{h}) as well as the efficiency (η^{e}_{ih}) of the units. A very high energy price (10000 €/MWh) is assumed for value of lost load (VOLL) in each system to avoid infeasibility in case that the generation cannot meet the demand.

The following subsections detail the energy balance for each system and the rest of the constraints are detailed in the appendix.

3.1. Power system

The electricity system representation includes generation plants (aggregated per technology type), cross-border transmission capacities, energy storage, including batteries, and pumped hydro. Electricity demand profiles are input to the model whereas electricity demand for electrolysis is generated endogenously. The electricity demand for electrolysis ($d^{eH_2}_{ip}$) is linked with hydrogen production via electrolysis ($q^{eH_2}_{ip}$) through efficiency of electrolysers (η^{eH2}_{i}). Eq. (5) provides the energy balance conditions for the power system and its dual variable provides the marginal cost of the power system ($price^{e}_{ip}$).

$$\sum_{oth,vre,hfp,nfp,gfp\in H}\left(q^{e}_{i(oth)p} + q^{e}_{i(vre)p} + q^{e}_{i(hfp)p} + q^{e}_{i(nfp)p} + g^{e}_{i(gfp)p}\right) + \sum_{r\in R}\left(ds^{e}_{irp} - ch^{e}_{irp}\right) + \sum_{i'\in J(i)}\left[flow^{e}_{i'ip} - flow^{e}_{ii'p}\right] + ens^{e}_{ip} = D^{e}_{ip} + d^{eH_2}_{ip}\left(price^{e}_{ip}\right) \;\forall i\in I, p\in P \tag{5}$$

The electricity generation of conventional units is constrained by

techno-economic parameters such as capacity (Q^{e}_{hi}), availability (AF^{e}_{ih}), efficiency (η^{e}_{ih}) as well as ramp rates (RR^{e}_{ih}), whereas generation from variable renewables depends on their capacity factor (CF^{e}_{ihp}). The electricity generation from hydrogen-fired power plants is linked with hydrogen demand for power generation through efficiency of hydrogen-fired turbines. The electricity generation from methane-fired power plants ($q^{e}_{i(nfp)p}, q^{e}_{i(gfp)p}$) is linked with methane demand for power generation through (d^{ge}_{ip}) efficiency of methane-fired turbines ($\eta^{e}_{i(nfp)}, \eta^{e}_{i(gfp)}$). The electricity storage operation is constrained by storage capacity (SC^{e}_{irp}), efficiency (EFF^{r}) as well as charging and discharging rates. The electricity flows are constrained by respective line capacities ($T^{e}_{ii'}$).

3.2. Hydrogen system

The hydrogen system representation includes grey and blue (gas reforming) and green hydrogen (electrolysis and biomass gasification) production, hydrogen storage and transport modules, as well as conversion of hydrogen into power. The hydrogen demand profiles for the residential, industry and transport sectors are input to the model whereas the hydrogen demand for power generation is endogenously generated. The hydrogen demand for power generation ($d^{H_2e}_{ip}$) is linked with electricity generation from hydrogen fired power plants ($q^{e}_{i(hfp)p}$) through efficiency of hydrogen-fired turbines ($\eta^{e}_{i(hfp)}$). Eq. (6) provides the energy balance conditions for the hydrogen system and its dual variable provides the hydrogen prices ($price^{H_2}_{ip}$).

$$q^{eH_2}_{ip} + q^{gH_2}_{ip} + q^{bgH_2}_{ip} + \sum_{f\in F}(e^{H_2}_{ifp} - inj^{H_2}_{ifp}) + \sum_{i'\in JL(i')}\left(tl^{H_2}_{i'ip} - tl^{H_2}_{ii'p}\right) + \sum_{i'\in JG(i)}\left(flow^{H_2}_{i'ip} - flow^{H_2}_{ii'p}\right) + ens^{H2}_{ip} = D^{H_2}_{ip} + d^{H_2e}_{ip} + d^{H_2g}_{ip}\left(price^{H_2}_{ip}\right)\forall i\in I, p\in P\# \tag{6}$$

Hydrogen production is constrained by the capacity of the units. The hydrogen production via electrolysis ($q^{eH_2}_{ip}$) is linked with electricity demand for electrolysis ($d^{eH_2}_{ip}$) through the efficiency of electrolysers (η^{eH2}_{i}). The hydrogen production via gas-reforming ($q^{gH_2}_{ip}$) is linked with methane demand for hydrogen production ($d^{gH_2}_{ip}$) through the efficiency of gas-reformers (η^{gH2}_{i}). Hydrogen flows ($flow^{H_2}_{ii'p}$) through the pipeline are limited to pipeline capacities ($TG^{H_2}_{ii'}$) while shipping volumes ($tl^{H_2}_{ii'p}$) are constrained by available liquefaction (TLG^{out}_{i}) and gasification (TLG^{in}_{i}) capacities.

3.3. Methane system

The methane system representation includes natural gas production, green gas production, liquid and pipeline transport capacities as well as storage capacities. The gas demand profiles for the residential, industry and transport sectors are input to the model, whereas methane demand for power generation as well as hydrogen production is endogenously generated. The methane demand for power generation (d^{ge}_{ip}) is linked to electricity generation methane-fired power plants($q^{e}_{i(nfp)p}, q^{e}_{i(gfp)p}$) through efficiency of methane-fired turbines ($\eta^{e}_{i(nfp)}, \eta^{e}_{i(gfp)}$). The methane demand for hydrogen production (d^{gH2}_{ip}) is linked to hydrogen production from gas-reforming ($q^{gH_2}_{ip}$) via efficiency of gas-reformers ($\eta^{gH_2}_{i}$). Eq. (7) provides the energy balance conditions for the methane system and its dual variable the methane prices ($price^{g}_{ip}$).

$$\sum_{z\in Z} q^{ng}_{zip} + q^{gg}_{ip} + q^{H2g}_{ip} + \sum_{i'\in JL(i')}\left(tl^{g}_{i'ip} - tl^{g}_{ii'p}\right) + \sum_{i'\in JG(i)}\left(flow^{g}_{i'ip} - flow^{g}_{ii'p}\right) + \sum_{n\in N}(e^{g}_{inp} - inj^{g}_{inp}) = D^{g}_{ip} + d^{ge}_{ip} + d^{gH2}_{ip}\left(price^{g}_{ip}\right)\forall i\in I, p\in P \tag{7}$$

Natural gas and green gas production is constrained by the capacity of the units. Methane generation through methanation process (q^{H2g}_{ip}) is linked with hydrogen demand for methane production ($d^{H_2g}_{ip}$) via efficiency of the methanation process ($\eta^{H_2g}_{i}$). Methane flows ($flow^{g}_{ii'p}$) through the pipeline are limited to pipeline capacities ($TG^{g}_{ii'}$) while shipping volumes ($tl^{g}_{ii'p}$) are constrained by available liquefaction ($TLNG^{out}_{i}$) and gasification ($TLNG^{in}_{i}$) capacities.

4. Case study: NL infrastructure outlook 2050

The Netherlands is participating in the global effort to develop a more sustainable, low-carbon energy system. In addition to the Paris climate agreement, it is fully committed to the European agreements on carbon reductions for 2030 and 2050. The 2019 Dutch national climate agreement between many organizations and companies, sets the vision for the energy system in 2050 and has specific targets and ambitions for 2030 for the built -environment, mobility, industry, agriculture and land use as well as the electricity sector [80]. Specifically, it aims to reduce greenhouse gas emissions in the Netherlands by 49% in 2030 compared to 1990 levels with specific commitments. The Dutch climate act aligns with the Paris climate agreement as well as the integrated national energy and climate plan. There is a broad consensus that hydrogen and carbon-free electricity system and transitioning away from natural gas will play an important role in the transition to carbon-neutrality. The Dutch climate agreement aims to scale up the production of renewable electricity to 84 TWh in 2030, of which 49 TWh will be generated from offshore wind and 35 TWh, from onshore wind and solar PV. Growth up to 60 GW of offshore wind capacity for 2050 is foreseen. It also recognizes the increased interactions between electricity and gas systems and identifies different flexibility options from interconnections, demand response, storage and controllable production. In 2019, the Dutch energy network operators Gasunie and Tennet jointly presented their first infrastructure outlook 2050 showing the requirements and limitations of a future energy system based on solar and wind energy [13]. As mentioned in the Dutch climate agreement, a follow-up Integrated Infrastructure Outlook 2030–2050 study is being conducted by the Dutch energy system operators [81].

The Infrastructure Outlook 2050 (IO2050) is a joint study by the electricity and gas network operators on the development of integrated infrastructure in the Netherlands and Germany in 2050 [13]. The starting point of IO2050 is the Paris agreement to achieve 95% CO_2 emission reduction in 2050 compared to 1990 levels [82]. The analysis is based on four scenarios, namely regional, national, international and general, reflecting different energy transition governance approaches based on different socio-economic and political factors. For the Netherlands, the scenarios for energy supply and demand are based on the study 'Grid for the Future' by CE Delft [69] designed to span extremities in future demand for energy transport infrastructure. The scenarios were developed using a variety of sector models and predominantly calibrated on consistency of the energy balance. The data associated with all these scenarios are available open-source at the website of the Energy Transition Model (ETM) [83].

For the proof-of-principle, the I-ELGAS model presented in Section 3 is tested using data from the regional scenario of the Infrastructure Outlook 2050 (herein after referred as IO2050). The regional scenario holds relatively high levels of domestic energy generation, conversion and storage and as such is well-suited for the developed integrated model. In other words, the regional scenario also represents the highest share of renewable energy supply, i.e. variable renewable capacities, hydrogen and green gas fired power generation capacities, as well as power to hydrogen capacities among the four scenarios. The spatial information for regionalization of the electricity, hydrogen and methane systems is provided by the Dutch transmission system operators TenneT (electricity) and Gasunie (gas). Finally, the amounts of electricity

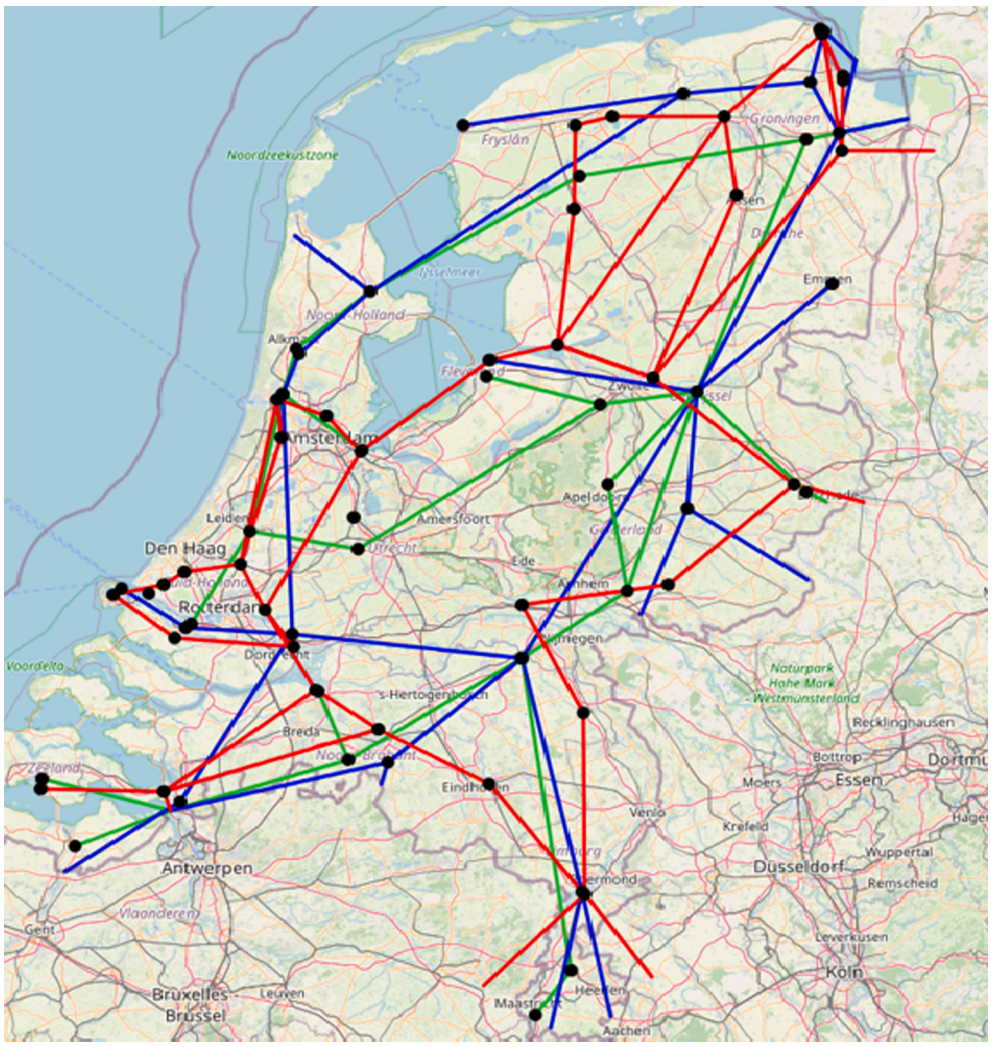

Fig. 3. Dutch transmission network topologies of electricity (red), hydrogen (blue) and methane (green) systems in 2050 [13,79].

import, hydrogen import and methane export were fixed at 0.16 TWh, 32.15 TWh and 19.41 TWh, respectively, to best match the IO2050 assumptions. Similar to IO2050 study, the carbon price is assumed to be 160 €/ton.

4.1. Network topologies

Fig. 3 illustrates the transmission network topologies for the Netherlands in IO2050 consisting of 34 electricity nodes, 22 methane nodes and 19 hydrogen nodes. This is an aggregated representation of the real situation with many more sub-stations. In addition, there are 5 electricity, 10 hydrogen, and 3 methane cross-border exchange nodes. In the regional scenario of IO2050, we did not model these nodes explicitly, but instead we considered electricity import of 0.16 TWh with import price of 400 €/MWh, hydrogen import of 32.15 TWh with import price of 4 €/MWh, methane export of 19.41 TWh and a biomass import price of 76 €/MWh to best match the IO2050 assumptions [13,69,83]. In addition, export of excess variable renewable generation is not permitted. As €/kg is common in the hydrogen sector, a conversion factor of approximately 39 kWh/kg (higher heating value) and 33 kWh/kg (lower heating value) can be used. Following IO2050, we also did not consider power lines smaller than 220 kV and pipelines with the pressure lower than 40 bar for electricity and methane grids, respectively. Regarding the interconnection between the electricity, methane and hydrogen nodes, capacities equivalent to that of conversion units are used as these were not provided in the IO2050 dataset. For example, the electricity interconnector capacities between electricity and hydrogen nodes (0.77–8.43 GW) is determined by the electrolyser capacity whereas hydrogen and methane pipeline capacities between electricity and methane (0.29–6.86 GW) or electricity and hydrogen nodes (0.44–1.32 GW) are determined by the capacities of methane or hydrogen-fired power plants, respectively.

4.2. Generation infrastructures

Based on IO2050 regional scenario data, the 2050 power generation mix in the Netherlands consists of offshore wind (26 GW), onshore wind (16 GW), solar PV (84 GW), hydrogen fired gas turbines (4.2 GW), methane-fired combined cycle gas turbines (8.4 GW), methane-fired combined heat and power as well as gas turbines (18.2 GW). Hydrogen is produced at the hydrogen nodes through electrolysers (75 GW) and biomass gasifiers (1.4 GW). These capacities are allocated to the respective hydrogen nodes as assumed in the IO2050 study.

4.3. Energy storage infrastructures

The residential electrical energy storage has an aggregated capacity of 5.93 GW with storage volume of 93 GWh. These capacities are allocated to the respective electricity nodes as assumed in the IO2050 study. Underground hydrogen storage with annual working gas capacity of 15

TWh is located in one of the hydrogen nodes whereas underground methane storage with annual working gas capacity of 25 TWh is located in one of the methane nodes, both in the north of the country. The initial and final storage level for the electrical energy storage is assumed to be 50%, whereas hydrogen and methane have initial and final storage levels of 10 TWh and 21 TWh, respectively, matching the IO2050 data.

4.4. Energy demand

I02050 assumes electricity demand of 171 TWh (including transport demand for electric vehicles), residential and industrial methane demand of 23 TWh as well as residential and industrial hydrogen demand of 80 TWh for the Netherlands. The flexible electricity demand for electrolysis as well as demand for methane and hydrogen for power generation are obtained endogenously in the model. The hourly national demand profiles as available in [83], are allocated to the respective electricity, hydrogen and methane nodes based on the IO2050 study.

5. Results

This section presents the results from the analysis of the regional baseline scenario of I02050, followed by some sensitivity analyses of this scenario.

5.1. Energy prices

Under the assumption of perfect competition, the shadow prices of energy balance equations [Eq.5- Eq.7] provide electricity, hydrogen and methane prices, respectively. Fig. 4 illustrates the distribution of hourly electricity, hydrogen and methane prices over the course of the simulated year in the IO2050 regional scenario, expressed in real values in Euros. The high share of solar and wind results in a high volatility and seasonality in notably electricity and hydrogen prices. An average annual electricity price of 148 €/MWh, an average annual hydrogen price of 63 €/MWh and an average annual methane price of 146 €/MWh results from the integral system optimization. Annual average prices for electricity, hydrogen and methane are relatively high due to the high biomass price assumption in the IO2050 study (76 €/MWh). The biomass is used to produce green gas via a fermentation process (with efficiency assumption of 54%) which in turn is used to run green-gas fired power units. Fig. 5 presents the average nodal electricity, hydrogen and methane prices over the course of the year. In the figure, three step changes for the electricity prices can be distinguished. These price levels correspond to methane-fired power plants, hydrogen-fired power plants and electricity generation from renewables (from high to low).

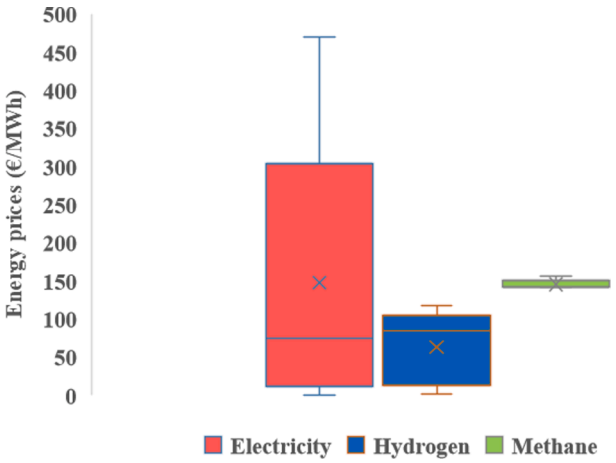

Fig. 4. Box-whisker plot of electricity, hydrogen and methane prices.

Fig. 5 illustrates that electricity and hydrogen prices are correlated and affect each other via additional electricity demand for electrolysis or additional hydrogen demand for power generation. The variation in hydrogen prices corresponds to hydrogen demand, storage, electrolysis using electricity-mix and renewables based electrolysis. The slight variation in the methane price is attributed to demand as well as transport and storage costs on top of the assumed constant price of 76 €/MWh for biomass.

5.2. Energy flows

The integrated model captures hourly flows for electricity, hydrogen and methane between the nodes. Fig. 6 illustrates three snapshots of archetypical hourly energy flows for variations in high and low renewable electricity production and electricity demand;

- Fig. 6a illustrates the snapshot of energy flows in hour 4044 (mid-June) when both variable renewable electricity production (108.7 GW) and exogenous electricity demand (20.5 GW) are high. In this hour, electricity demand, including the endogenous electricity demand for electrolysis (35.1 GW) is entirely supplied by renewable electricity generation and the excess electricity generation is stored in batteries (5.9 GW) and as hydrogen (22 GW). This leads to loading in power lines from offshore wind locations towards load centres, excessive curtailment of wind (47.3 GW) as well as flows towards hydrogen and methane storage nodes (located in the north of the country). The storage of hydrogen (22 GW) and methane (5.6 GW) can be attributed to excess renewable electricity generation with low gas demand in other sectors in mid-June (notably hour 4044).
- Fig. 6b illustrates the snapshot of energy flows in hour 954 (mid-February) when the supply of variable renewables (1.2 GWh) is very low and exogenous electricity demand (36.8 GWh) is very high. In such an hour, there is no endogenous electricity demand for electrolysis and the residual electricity demand is supplied by hydrogen-fired power plants (3.7 GWh), methane-fired power plants (20.9 GWh), electricity storage (5.9 GWh) and electricity import (5 GWh). Therefore, Fig. 7b slightly lower loading in power lines (especially north to south) as well as slightly higher flows from hydrogen (17.6 GWh) and methane storage (52.4 GWh) nodes to generation nodes where hydrogen and methane fired power plants are located.

5.3. Energy balance

The integrated model provides hourly energy balances for electricity, hydrogen and methane at respective nodes. The annual energy balance for electricity in IO2050is illustrated in Fig. 7. Some 39% of overall electricity demand results from electrolysis and electricity storage while some 58% of overall demand results from exogenous electricity demand. As export to other countries is not permitted, approximately 3.7% of variable renewable has to be curtailed.

Fig. 8 illustrates the annual energy balances of the hydrogen and methane system in IO2050. Some 27% of the annual hydrogen demand is required for power generation while 73% of the annual hydrogen demand originates from the exogenously assumed residential and industrial demand for hydrogen. In case of methane, demand for power generation is twice as high as the exogenously assumed residential and industrial demand for methane. A significant hydrogen and methane demand for storage is required to cover for seasonal imbalances between supply and demand, respectively spanning 48% and 35% of the annual hydrogen and methane demand.

5.4. System allocation and cross-sector utilization

The integrated model provides an optimal hourly dispatch for generation, conversion, storage and transport units. Driven by the solar and wind generation as well as demand profiles, the model calculates hourly

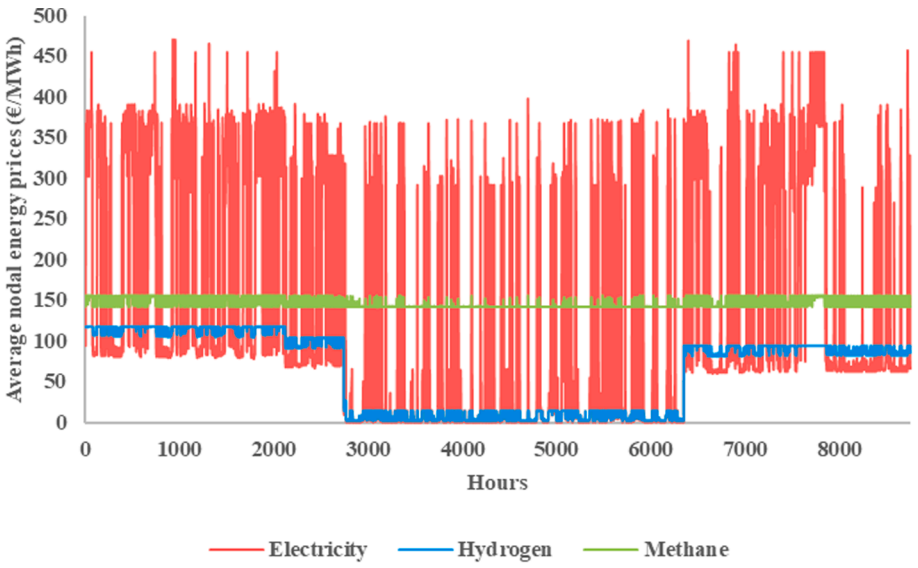

Fig. 5. Average nodal electricity, hydrogen and methane prices.

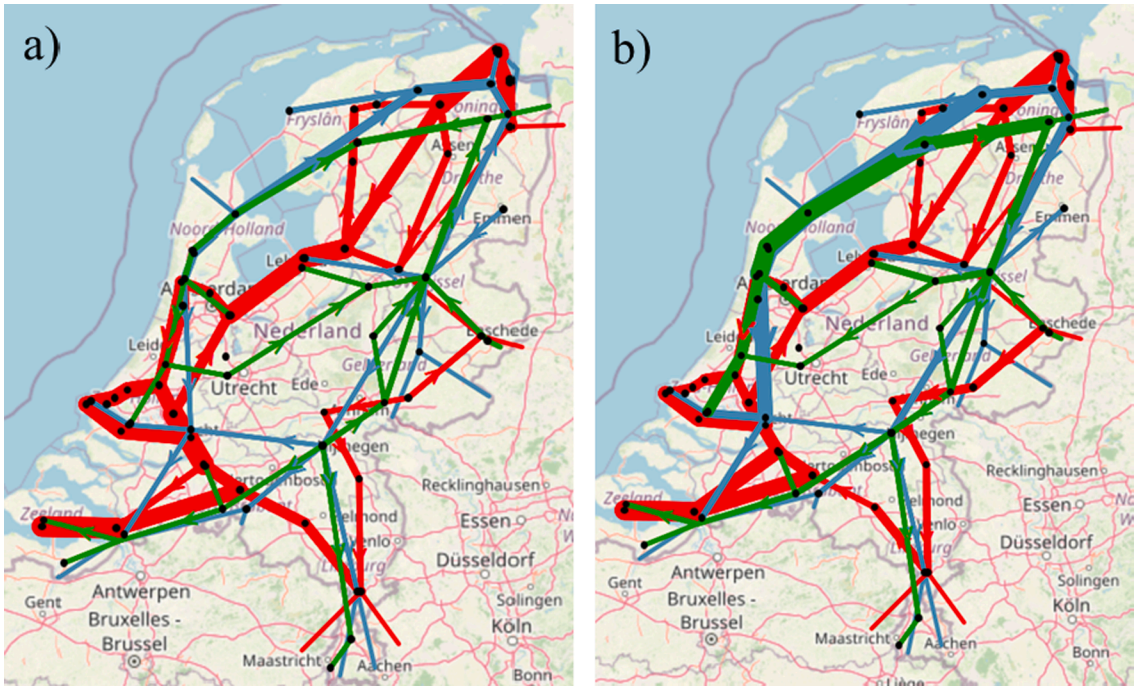

Fig. 6. Snapshot of electricity (red), hydrogen (blue) and methane (green) flows, a) high variable renewable electricity production and electricity demand (hour 4044) and b) very low variable renewable electricity production and very high electricity demand (hour 954).

supply profiles for hydrogen production via electrolysis and biomass gasification, green gas production via fermentation, and power generation from hydrogen and methane-based power plants. The full load hours of selected generation and conversion technologies are provided in Fig. 9. These full load hours should be understood in relation to the installed capacity of generation and conversion units as presented in Section 4.2. It is worth mentioning here that in the IO2050 scenario, solar and wind generation is sufficient for 608 h in a year to cover the entire electricity demand including the demand for electrolysis and electricity storage charging. The methane-fired units become the marginal generating unit for 2940 h.

Fig. 10 shows the hourly storage level of electricity, hydrogen and methane. Table 1 presents storage capacity, annual storage volume and full cycle equivalent for each storage type. Frequent short-term cycles are observed in electricity storage as it balances short-term fluctuations in solar and wind, whereas a seasonal cycle is observed in methane and hydrogen storage as these mainly balance long-term fluctuations in supply and demand of hydrogen and methane, respectively. Yet, hydrogen storage also provides short-term flexibility throughout the year. It is interesting to note the smoothness of the methane storage level in summer months. This is attributed to the assumption of relatively high prices of green gas production, so that the methane storage mainly provides flexibility to the system during winter months (when the amount of variable renewable electricity in the system is relatively low). Due to the abundance of low-cost variable renewable electricity for hydrogen production, hydrogen storage provides both short-term and long-term flexibility to the system.

As shown in Fig. 1, the electricity, hydrogen and methane systems

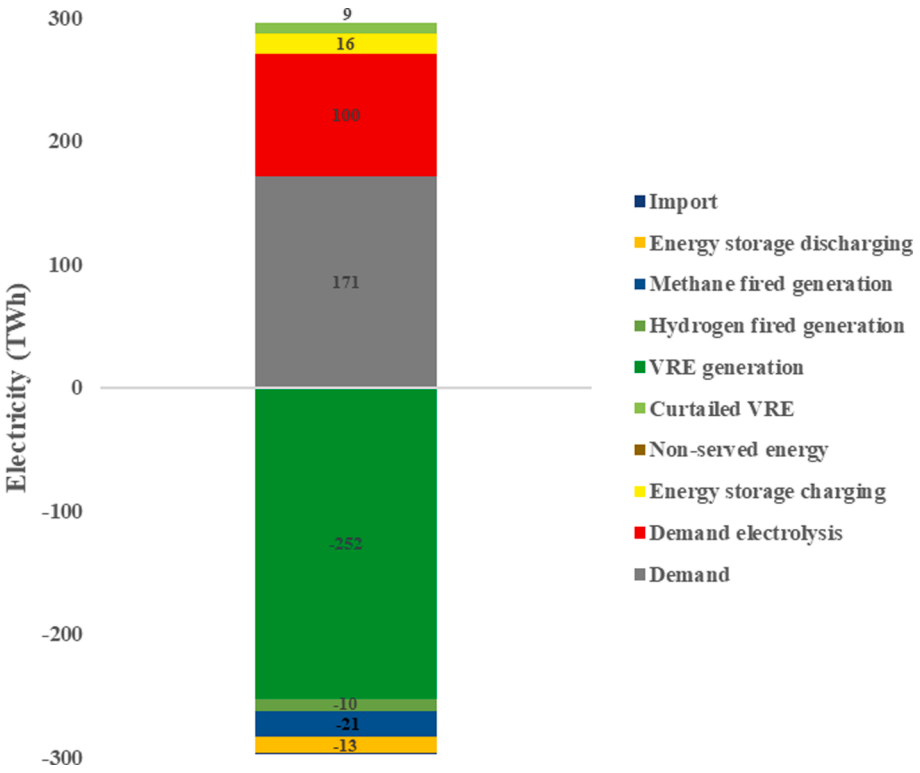

Fig. 7. Annual electricity balance in the Netherlands (IO2050).

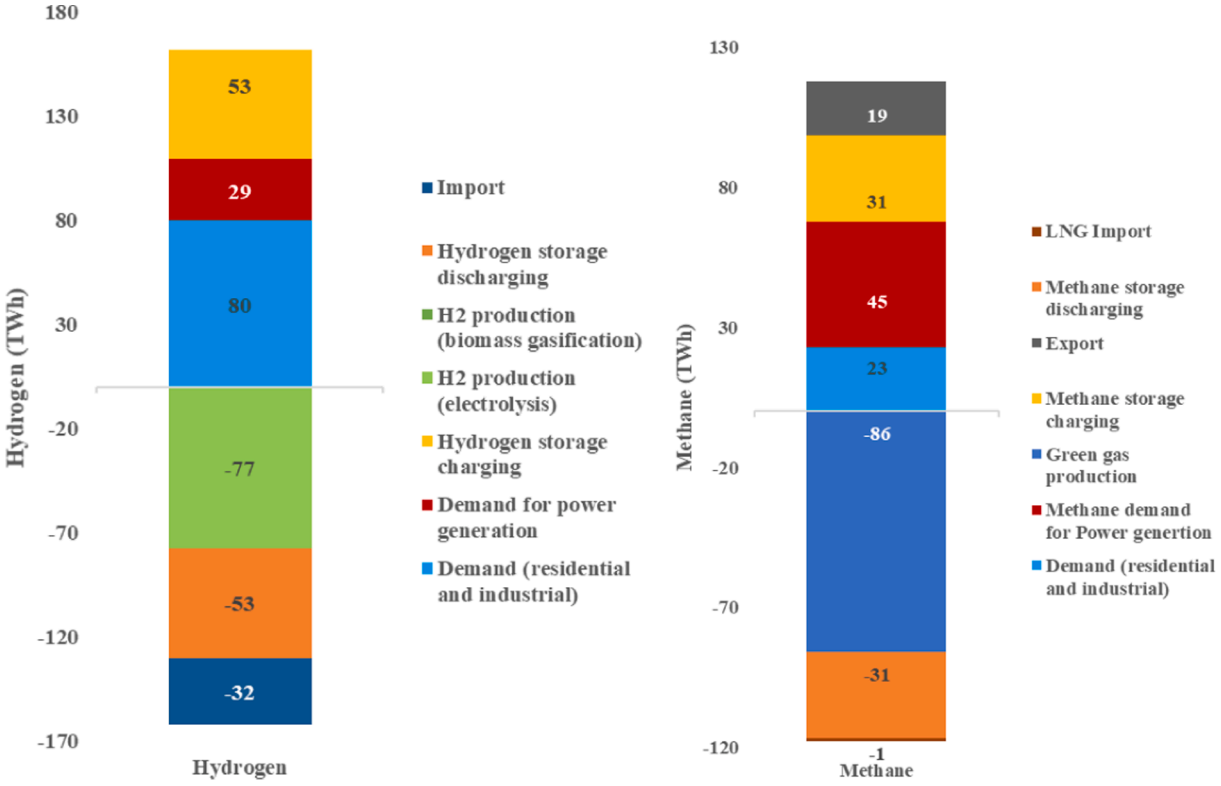

Fig. 8. Annual hydrogen and methane balance in the Netherlands (IO2050).

are interlinked. Fig. 11 presents the exchanges between these sub-systems. Based on the IO2050 scenario, the hydrogen system utilizes 100 TWh of electricity to produce hydrogen via electrolyser units, and 29 TWh of hydrogen is used in the power system to generate electricity via hydrogen-fired power plants. At the same time, 45 TWh of methane is utilized by the power system to generate electricity via methane-fired power plants.

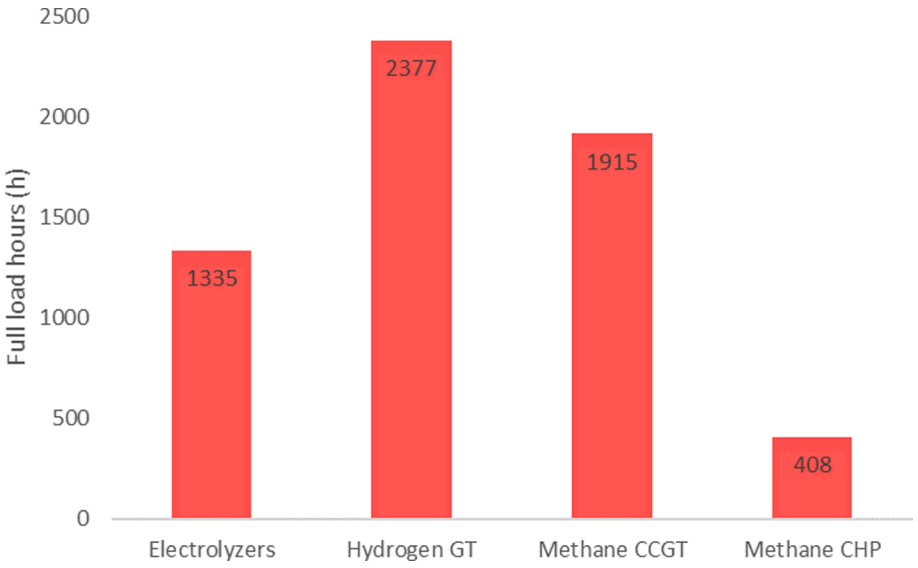

Fig. 9. Full load hours of generation and conversion technologies.

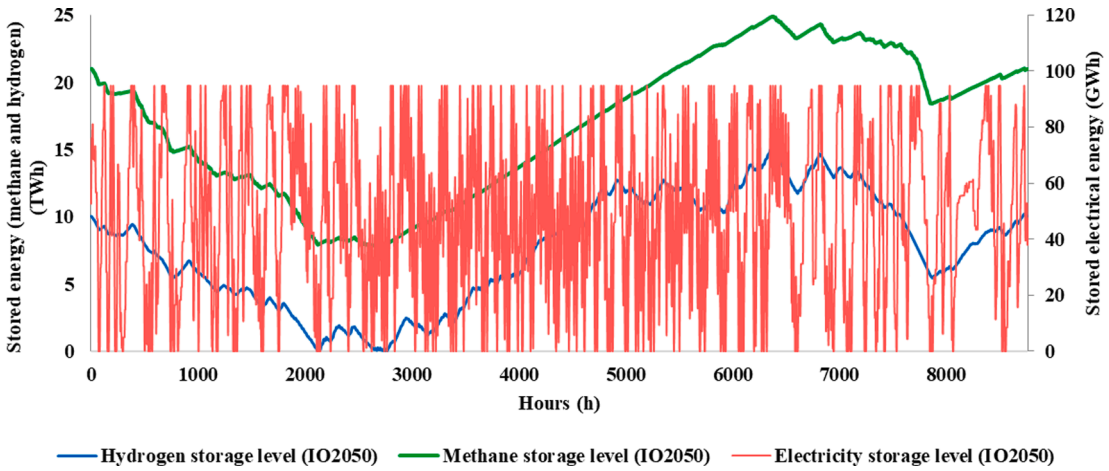

Fig. 10. Hourly storage level of electricity, hydrogen and methane.

Table 1
Electricity, hydrogen and methane storage characteristics.

Storage type	Storage capacity(TWh)	Annual storage volume (TWh)	Annual full cycle equivalent (cycles)
Electricity	0.093	15.67	168.5
Hydrogen	15	52.72	3.5
Methane	25	30.51	1.22

5.5. Sensitivity analysis

The present energy landscape is changing rapidly. As the costs are decreasing, solar PV, wind turbines and electrolysers are being added to the energy systems at unprecedent rates. Due to energy efficiency measures, demand might decrease but at the same time application areas for the energy vectors are also widening, for example, increasing electrification of different end use sectors and hydrogen-based mobility. The IO2050 scenario was designed with energy balance as a basis without an integral framework for market pricing. The scaling of 1) wind/solar, 2) conversion (electrolyzers) and 3) electricity/hydrogen demand was never balanced in terms of cost-optimal system development. To address these potential issues, in addition to the baseline IO2050 regional scenario, some sensitivity analyses are performed by varying selected parameters which are considered as main drivers of the I-ELGAS model and to test their impact on the results, as illustrated in Table 2. One parameter is varied at a time, leading to 7 sensitivity runs in total. The rest of the input data is assumed to be the same. Although, it would be generally interesting to test the impact of these runs on GHG emissions, the I02050 study assumes that the future energy system will be emission free with green hydrogen, bio liquified gas and green gas. Hence, total GHG emissions are zero in all cases and, therefore, they are not included in the results of the sensitivity analyses discussed below.

5.5.1. Energy prices

As illustrated in Fig. 12, both the increase in variable renewable capacities and decrease in energy demand lead to lower average energy prices. The 25% increase in variable renewable capacities leads to a 91% decrease in average hydrogen prices, 38% decrease in average electricity prices and 0.6% decrease in average methane prices. At the same time, a 10% increase in variable renewable capacities leads to a 60% decrease in average hydrogen prices, 19% decrease in average electricity prices and 0.3% decrease in average methane prices. On the other hand, a 10% decrease in energy demand reduces electricity prices by 32%, hydrogen prices by 89% and methane prices by 0.57%. While 25% simultaneous decrease in electricity, hydrogen and methane demand leads to 93% decrease in average hydrogen prices, 55% decrease in average electricity

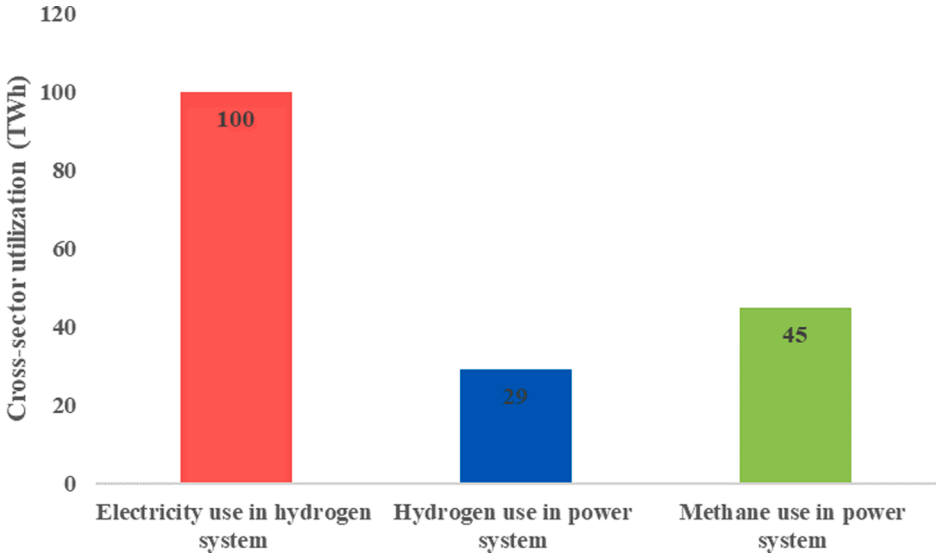

Fig. 11. Cross-sector utilization of energy vectors.

Table 2
Sensitivity analysis setup and assumptions.

Parameters	Baseline (IO2050)	Sensitivity	Values for sensitivity analysis
Variable renewable capacities	**126**	**+25%**	**157.5**
Onshore wind (GW)	26		33
Offshore wind (GW)	16		20
Solar PV (GW)	84		105
Variable renewable capacities	**126**	**+10%**	**138.6**
Onshore wind (GW)	26		28.6
Offshore wind (GW)	16		17.6
Solar PV (GW)	84		92.4
Demand (TWh)	**274**	**−25%**	**205.5**
Electricity demand (TWh)	171		128.25
Hydrogen demand (TWh)	80		60
Methane demand (TWh)	23		17.25
Demand (TWh)	**274**	**−10%**	**246.6**
Electricity demand (TWh)	171		153.9
Hydrogen demand (TWh)	80		72
Methane demand (TWh)	23		20.7
Biomass price (€/MWh)	**76**	**+25%**	**95**
Biomass price (€/MWh)	**76**	**−25%**	**57**
Biomass price (€/MWh)	**76**	**−50%**	**38**

prices and 2% decrease in average methane price. The 25% changes in biomass prices almost proportionally affect the average electricity, hydrogen and methane prices as biomass indirectly sets the prices for 2990 h in the year and the merit order of green-gas fired units remains mostly unaffected due to 25% changes in biomass prices While 50% decrease in biomass prices leads to 44% decrease in electricity prices (methane-fired units are marginal for 3123 h), 49% decrease in hydrogen prices and 47% decrease in methane prices.

5.5.2. System allocation and cross-sector utilization

Fig. 13 illustrates the changes in cross-sector utilization of electricity, hydrogen, and methane. The 25% increase in variable renewables leads to 30% lower utilization of methane in power generation, while 25% decrease in conventional demand leads to 68% lower utilization of methane in the power system. A 10% increase in variable renewable capacities leads to 5.5% higher electricity use in hydrogen system, 14.5% higher hydrogen use in power system and 9.6% lower methane use in power system. As the system is delimited, 25% increase in variable renewables leads to only slightly lower utilization of electricity use in electrolysis (0.25% lower) which in turns is due to lower hydrogen demand for hydrogen-fired power generation (0.65% lower). It is interesting to note that both 10% reduction in demand and 10% increase in variable renewable capacity leads to increase in hydrogen use in power system and decrease in methane use in power system. This is due to lower hydrogen price in both cases due to lower demand or increase availability of renewables. The surplus electricity is converted into hydrogen and used to fire flexible hydrogen turbines. As IO2050 scenario is delimited, this is however not the case when demand is reduced by 25% and variable renewables capacities are increased by 25%, as renewable electricity is directly used to supply demand without intermediate conversion into hydrogen. The 25% decrease in demand leads to 31.5% lower electricity use in the hydrogen system which can be attributed to 14.6% lower hydrogen use in the power system. As 25% changes in biomass prices do not lead to significant changes in cross-sector utilization, it is not visualized in Fig. 13. While 50% reduction in biomass prices leads to 2.3% higher electricity use in hydrogen system, 7.3% higher hydrogen use in power system and 7.2% higher methane use in power system.

The variation in full load hours of generation and conversion technologies is provided in Fig. 14. The 25% increase in variable renewables leads to 0.25% lower dispatch of electrolysers, 0.66% lower dispatch for hydrogen-fired turbines, 31% lower dispatch for methane fired CCGT and 27% lower dispatch for methane fired CHP units. At the same time, a 10% increase in variable renewable capacities leads to 5.5% higher deployment of electrolysers, 14.5% higher deployment of hydrogen-fried turbines, 14.8% lower deployment of methane CCGT and 28.5% lower deployment of methane CHP. On the other hand, 25% decrease in demand leads to 31% lower dispatch for electrolysers, 15% lower dispatch for hydrogen fired turbines, 60% lower dispatch for methane-fired CCGT and 87% lower dispatch for methane-fired CHP. As the study is performed in a delimited system, the excessive variable renewables generation and lower demand also lead to higher curtailment of wind and solar. As a 25% reduction in biomass prices do not lead to significant changes in system allocation, it is not visualized in Fig. 14. While 25% increase in biomass prices leads to 0.82% lower deployment of methane-fired CCGT units and 2.01% higher deployment of Methane-

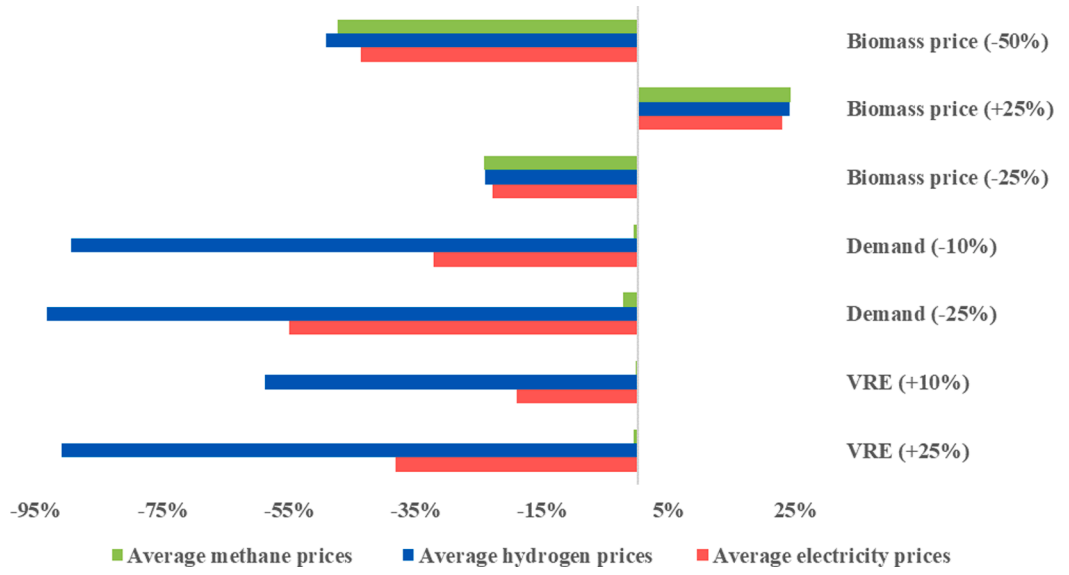

Fig. 12. Sensitivity analysis on average energy prices.

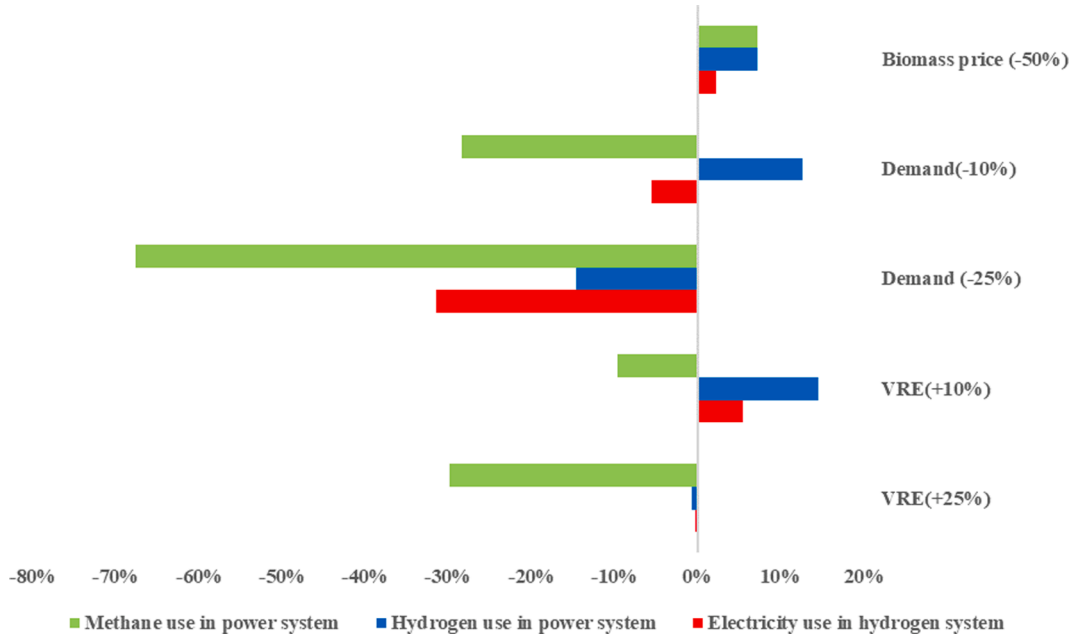

Fig. 13. Sensitivity analysis of cross-sector utilization of energy vectors.

fired CHP units. At the same time, 50% lower biomass prices leads to 2.31% higher deployment of electrolyzers, 7.31% higher deployment of hydrogen-fired turbines, 3.55% higher deployment of methane-fired CCGT and 19.82% lower deployment of Methane CHP units. It is interesting to note that both when biomass prices is reduced by 50% and variable renewable capacities are increased by 10%, hydrogen deployment is higher as it provides flexibility to the delimited system.

Fig. 15 shows the hourly variation in the deployment of hydrogen and methane storage for the IO2050 baseline, 25% reduction in demand and 25% increase in variable renewables. The higher renewable capacities lead to an increase in variable renewable electricity which in turn reduces the demand for hydrogen and methane based power generation, leading to aggregated lower deployment of both hydrogen (48.5 TWh) and methane storage (21.7 TWh) compared to the IO2050 baseline of 52.7 TWh and 30.5 TWh of hydrogen and methane storage respectively. The 25% lower energy demand also leads to significantly lower deployment of both hydrogen (34.7 TWh) and methane storage (7.1 TWh) than the base case. Although not visualized in Fig. 15, the higher share of renewables increases the electricity storage deployment by 1.6 TWh and the decrease in energy demand increases the deployment of electricity storage by 0.3 TWh.

To summarize, the increase in variable renewable capacities or decrease in demand has similar impact on energy prices. Both have most impact on hydrogen prices, followed by electricity prices and the impact on methane prices is not significant. A decrease in energy demand has a more significant impact on cross sector utilization as well as system allocation than the increase in variable renewable capacities. As the system is delimited, it is interesting to note that smaller perturbation (±10%) variable generation capacities lead to higher interactions between hydrogen and power system than the larger perturbation (±25%). However, hydrogen storage deployment is less affected than the methane storage as excess electricty in both sensitivity cases could be

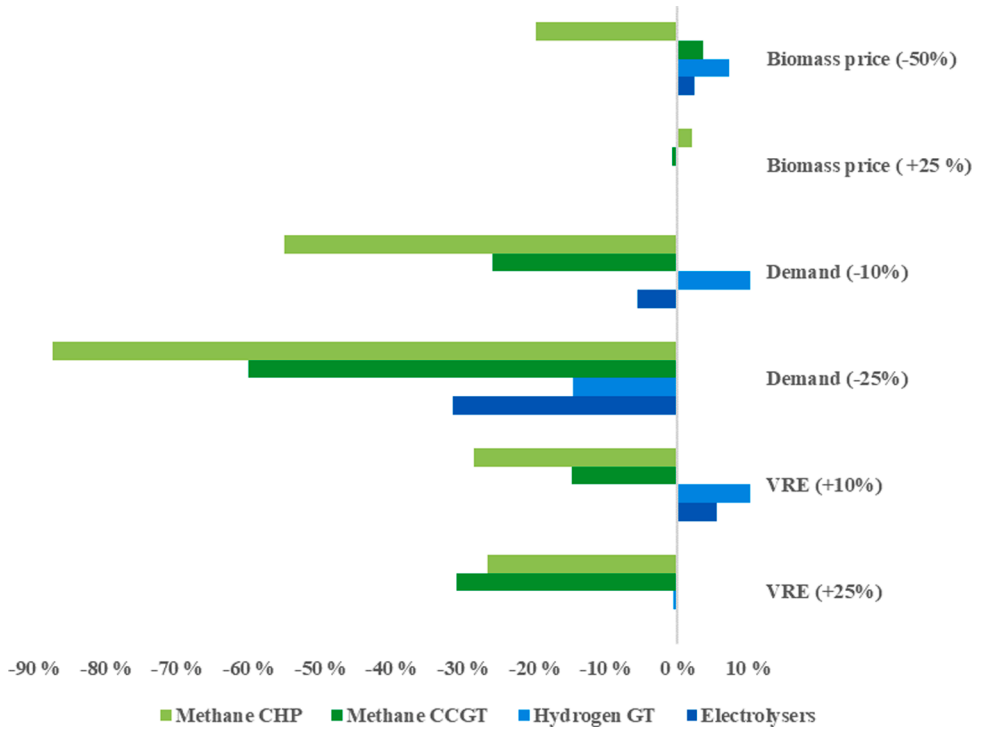

Fig. 14. Sensitivity analysis on full load hours of generation and conversion technologies.

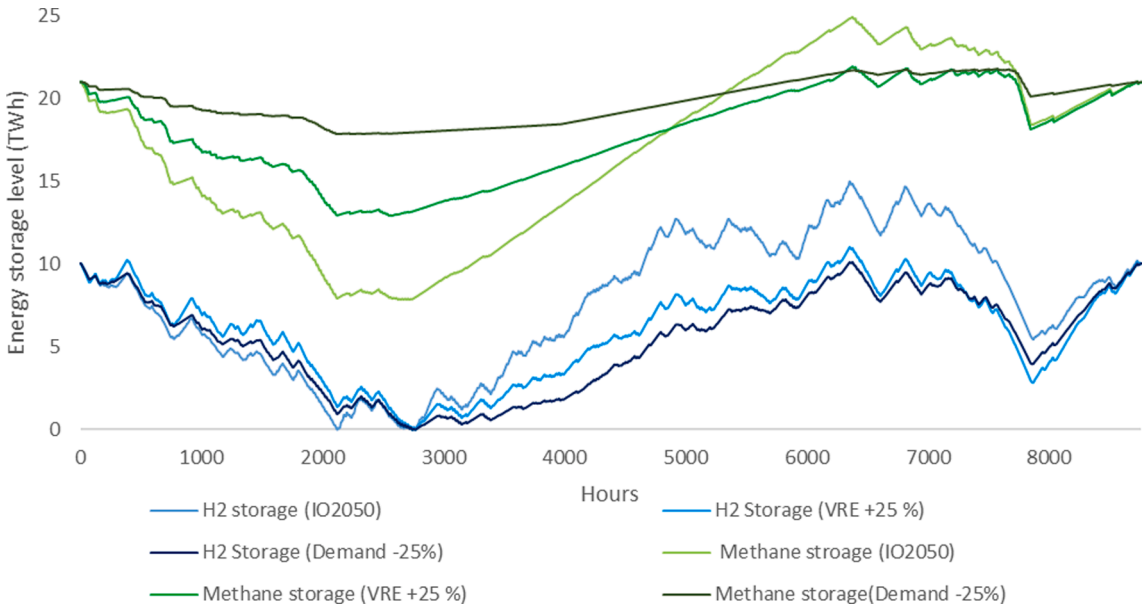

Fig. 15. Sensitivity analysis on methane and hydrogen storage level.

converted to hydrogen molecules and stored. Biomass prices (±25%) proportionally impact the commodities prices and do not have significant impact on cross-sector utilization as well as system allocation. This changes, however, when biomass prices is further reduced (-50%).

6. Discussions

Increasing deployment of conversion technologies such as electrolysers, gas reformers, natural gas-fired power plants, hydrogen-fired power plants and hybridization of final demand may lead to increasingly coupled electricity, hydrogen and gas markets and systems. With increasing renewables as well as electrification and decarbonization of the energy-demand sectors, the interactions between these markets and systems will further increase in the future. There is widespread consensus that further integration and coupling of electricity, hydrogen and methane systems are important for the decarbonization of the energy system. The whole energy system is expected to benefit from it in terms of flexibility, avoiding unnecessary network expansion and, in general, efficiency. Yet, integrated operation of systems which are designed for individual operation will not be without challenges as operational decisions for one system will impact other systems. This necessitates an integrated assessment of these markets and systems.

This article formulates an integrated electricity and (renewable) gas model to mainly study price and volume interactions on an hourly basis,

also considering associated infrastructures, ramp rates, energy storage (gas, electricity and hydrogen) as well as variability in supply and demand. The integrated model is formulated as a single linear programming optimization problem which finds the market equilibrium of the integrated electricity, hydrogen and gas markets assuming perfect competition. The integrated model takes into account short and long term price and volume effects, differentiating in detail the flexibility capabilities of different sources in electricity, hydrogen and methane systems. The integrated model also allows for a more detailed analysis of energy systems on a large geographical and temporal scale.

Similar to other scenario studies, this research is not without limitations. As the research was conducted in a delimited system (i.e. without demand response or foreign trade changing total domestic electricity demand), an increased share of variable renewables leads to excessive curtailment of variable renewables. Moreover, the surplus renewable electricity cannot be converted to molecules because there is no additional demand for these molecules. As import and export amounts of energy are fixed to best match the Infrastructure Outlook 2050 assumptions, this excess in variable renewables cannot be used for export and also the excess production of variable renewables abroad cannot be imported at a cheaper import price. Moreover, the residential and industrial demand for electricity, hydrogen and methane is fixed without room for flexibility. The only demand side flexibility comes from electricity demand for hydrogen production, as well hydrogen and methane demand for electricity production. These imposed limitations to best match the Infrastructure Outlook 2050 scenario lead to higher energy prices. Yet, it is important to understand that the goal of this scenario analysis was to establish a cross validation with the Infrastructure Outlook 2050 study, not to establish a realistic scenario.

Another shortcoming arises from the LP formulation: although it allows the model to increase the temporal (with right storage and other assets deployment) and spatial descriptions of the model, it also prevents it from including many important analytical elements and their non-linear constraints, such as detailed operation 1) of thermal generation, e.g., startup/shutdown, minimum output, minimum up/down time constraints, and 2) of gas-flow dynamics of the gaseous networks. As the main assumption is perfect competition, the integrated model is not suitable to use for market power issues.

Future research should focus on addressing these shortcomings and should also include optimal capacity expansion planning, ideally including the non-linear constraints as those mentioned above. Besides these, the shadow prices of capacity constraints (generation capacity, transmission capacity etc.) have also economic meaning. They are called scarcity rents for generation capacity or congestion rents for transmission capacity. When these capacities are running at 100%, they are positive and are equal to what operators of these capacities get on top of their short-run marginal cost. The annual scarcity rent could be compared to the annual investment costs and used to assess business cases for investing in these capacities. Since we are not discussing investment decisions at all in this article, this should be considered in the future work. Also the buffer storage of hydrogen and methane in the line pack as well as storage losses should be considered. Different applications of hydrogen may require different qualities (purity) and these require additional quality conversions and/or independent storage and transport systems. Future research should therefore also study the regulatory and policy implications of integrated operation of electricity, hydrogen and methane infrastructures. The integrated model can be used as a tool by market parties, network operators, policy makers and regulators to capture implications of possible techno-economic and institutional developments in one system for the operation of others.

7. Conclusion

The power and (renewable) gas markets are interdependent due to multiple conversion technologies such as electrolysers, hydrogen and methane fired generation units, gas reformers and methanation units. This makes the integrated analysis of power and (renewable) gas markets important. This article provides a modelling framework for integrated electricity, hydrogen and methane systems with high spatio-temporal granularity and considering interdependencies and linkages between these systems. To our knowledge, none of the existing integrated (renewable) gas and electricity market models, that can capture the short-term price and volume effects of all three markets (electricity, methane and hydrogen) and differentiates the flexibility capabilities of different sources on this level of detail.

The analysis presented in this article shows that the price–volume interaction between electricity, methane and hydrogen markets become stronger with increasing variable renewables generation. The interweaving of electricity, methane and hydrogen infrastructures via conversion technologies (e.g., electrolysers), power plants (gas and hydrogen-fired), gas reformers and methanation units provide the flexibility needed by the future energy system. For example, for the Infrastructure Outlook 2050 study, with the increase of variable renewable electricity, the power generation from methane and hydrogen fired power plants decreases to absorb increased variable renewable electricity. This leads to lower demand for methane and hydrogen for power generation, which in turn leads to lower deployment of methane and hydrogen storage. The deployment of electrical energy storage increases to provide short-term flexibility to the power system. Flexibility from electric batteries balances daily variation of solar and wind whereas methane and hydrogen storage mostly balances seasonal variation of demand and supply. Due to the availability of low-cost variable renewables, the combination of power-to-hydrogen and hydrogen-to-power provides also short-term flexibility to the energy system.

Sensitivity analysis reveals that the increase in variable renewable capacities or decrease in demand has a significant impact on electricity and hydrogen prices. The impact is most significant on hydrogen prices, followed by electricity prices and the impact on methane prices is least significant. A decrease in energy demand has a more significant impact on cross sector utilization as well as system allocation than the increase in variable renewable capacities. Moreover, as excess electricity from variable renewables can be converted into hydrogen and hydrogen can in turn be used to produce electricity, hydrogen storage deployment is less affected than the methane storage. As methane fired units often (2940 h) set the peak electricity prices, biomass prices proportionally impacts the electricity, methane and hydrogen prices but do not have significant impact on cross-sector utilization as well as system allocation.

As mentioned in Section 3, an extended version of the model covering North Sea Countries is already available and in future the model will be further extended to cover the European scale and analyse important issues such as role of hydrogen and methane in European energy system under rapidly increasing shares of variable renewable generation.

CRediT authorship contribution statement

Binod Koirala: Conceptualization, Investigation, Methodology, Data curation, Visualization, Writing - original draft, Writing - review & editing. **Sebastiaan Hers:** Conceptualization, Methodology, Writing - review & editing, Supervision, Validation, Aquisition. **Germán Morales-España:** Conceptualization, Investigation, Writing - review & editing. **Özge Özdemir:** Conceptualization, Supervision, Writing - review & editing, Validation. **Jos Sijm:** Methodology, Writing - review & editing, Supervision, Validation. **Marcel Weeda:** Supervision, Validation.

Declaration of Competing Interest

The authors declare that they have no known competing financial interests or personal relationships that could have appeared to influence the work reported in this paper.

Acknowledgement

The authors are thankful to the Dutch transmission system operators Gasunie and TenneT for sharing the data related to spatial distribution of generation, demand and infrastructures for electricity, hydrogen and methane systems as well as their expert feedback to the model results. We also acknowledge the support of the Energy System Description Language (ESDL®) team, especially Edwin Matthijssen, in applying mapeditor® to geographically visualize the energy flows.

Appendix A

As an extension of the model formulation presented in Section 3, this appendix provides the rest of the model formulation for the integrated electricity, methane and hydrogen market model.

Eq. (8) shows that the hydrogen demand for power generation ($d_{ip}^{H_2 e}$) is linked with electricity generation from hydrogen fired power plants ($q_{i(hfp)p}^{e}$) through efficiency of hydrogen-fired turbines ($\eta_{i(hfp)}^{e}$).

$$d_{ip}^{H_2 e} = \sum_{h \in hfp} \frac{q_{ihp}^{e}}{\eta_{ih}^{e}} \quad \forall i \in I, p \in P \tag{8}$$

Eq. (9) indicates that the electricity generation from methane-fired power plants ($q_{i(nfp)p}^{e}, q_{i(gfp)p}^{e}$) is linked with methane demand for power generation (d_{ip}^{ge}) through efficiency of methane-fired turbines ($\eta_{i(nfp)}^{e}, \eta_{i(gfp)}^{e}$).

$$d_{ip}^{ge} = \sum_{h \in nfp, gfp} \frac{q_{ihp}^{e}}{\eta_{ih}^{e}} \quad \forall i \in I, p \in P \tag{9}$$

As illustrated in Eq. (10), the methane demand for hydrogen production (d_{ip}^{gH2}) is linked to hydrogen production from gas-reforming ($q_{ip}^{gH_2}$) via efficiency of gas-reformers ($\eta_{i}^{gH_2}$).

$$d_{ip}^{gH2} = \frac{q_{ip}^{gH2}}{\eta_{i}^{gH2}} \quad \forall i \in I, p \in P \tag{10}$$

The electricity demand for electrolysis ($d_{ip}^{eH_2}$) is linked with hydrogen production via electrolysis ($q_{ip}^{eH_2}$) through efficiency of electrolysers (η_{i}^{eH2}), see Eq. (11).

$$d_{ip}^{eH_2} = \frac{q_{ip}^{eH_2}}{\eta_{i}^{eH2}} \quad \forall i \in I, p \in P \tag{11}$$

As shown in Eqs. (12)–(15), the marginal cost of electricity generation from a power plants depends on fuel prices, efficiency of the power plants, emission factor, emission costs and operation and maintenance costs. Green gas, hydrogen and natural gas prices are determined endogenously in the model.

$$c_{ihp}^{e} = \left(\frac{FP_{ihp}^{e}}{\eta_{ih}^{e}} + \frac{\Theta_{h}^{e}.PCO2}{\eta_{ih}^{e}} + OM_{ih}^{e} \right) \quad \forall i \in I, h \in OTH, p \in P \tag{12}$$

$$c_{ihp}^{e} = \left(OM_{ih}^{e} \right) \quad \forall i \in I, h \in HFP/GFP, p \in P \tag{13}$$

$$c_{ihp}^{e} = \left(\frac{\Theta_{h}^{e}.PCO2}{\eta_{ih}^{e}} + OM_{ih}^{e} \right) \quad \forall i \in I, h \in NFP, p \in P \tag{14}$$

Eqs. (15)–(16) provides the marginal costs of gas-reformers and electrolyser units whereas the electricity and methane prices are determined endogenously in the model.

$$c_{ip}^{gH2} = \left(\frac{\Theta^{gH2}.PCO2}{\eta_{i}^{gH_2}} + OM_{i}^{gH2} \right) \quad \forall i \in I, p \in P \tag{15}$$

$$c_{ip}^{eH2} = \left(OM_{i}^{eH2} \right) \quad \forall i \in I, p \in P \tag{16}$$

Eqs. (17)–(20) provide the constraints for electricity generators. Electricity generation depends on availability of the generators, capacity factors (for variable renewables) and ramp rates.

$$g_{ihp}^{e} \leq AF_{ih}^{e}.G_{hi}^{e} \quad \forall i \in I, h \in H, p \in P \tag{17}$$

$$g_{ihp}^{e} \leq CF_{ihp}^{e}.G_{hi}^{e} \quad \forall i \in I, h \in VRE, p \in P \tag{18}$$

$$-RR_{ih}^{e} \leq g_{ihp+1}^{e} - g_{ihp}^{e} \leq RR_{ih}^{e} \quad \forall i \in I, h \in H, p \in P \tag{19}$$

$$g_{ihp}^{e} \geq 0 \quad \forall i \in I, h \in H, p \in P \tag{20}$$

Equations 21–22 provide the constraints for electricity transmission.

$$flow_{ii'p}^{e} = B_{ii'}(\theta_i - \theta_{i'}) \quad \{\forall i' \in J(I)\} \quad \forall p \in P \tag{21}$$

where $B_{ii'}$ is the susceptance of line ii' and θ_i is the voltage angle at bus i. The DC power flow equations are mentioned here but not yet used in this model.

$$flow^{e}_{ii'p} \leq T^{e}_{ii'} \quad \{\forall i' \in J(I)\}\forall p \in P \tag{22}$$

Equations 14–20 provide constraints for the operation of electric energy storage.

$$ch^{e}_{irp} \leq PS^{e}_{ir} \quad \forall i \in I, r \in R, p \in P \tag{23}$$

$$ds^{e}_{irp} \leq PS^{e}_{ir} \quad \forall i \in I, r \in R, p \in P \tag{24}$$

$$sol^{e}_{irp} = \mathrm{I}SC^{e}_{r0} + ch^{e}_{irp}.EFF^{r} - \frac{ds^{e}_{irp}}{EFF^{r}} \quad \forall i \in I, r \in R, p = 1 \tag{25}$$

$$sol^{e}_{irp} = sol^{e}_{irp-1} + ch^{e}_{irp}.EFF^{r} - \frac{ds^{e}_{irp}}{EFF^{r}} \quad \forall i \in I, r \in R, p > 1 \tag{26}$$

$$sol^{e}_{irp} = \mathrm{I}SC^{e}_{r0} \quad \forall i \in I, r \in R, p = T \tag{27}$$

$$sol^{e}_{irp} \leq SC^{e}_{ir} \forall i \in I, r \in R, p \in P \tag{28}$$

$$ch^{e}_{irp}, ds^{e}_{irp}, sol^{e}_{irp} \geq 0 \quad \forall i \in Ir \in Rp \in P \tag{29}$$

Eqs. (30)–(33) present capacity constraints for hydrogen production.

$$q^{gH_2}_{ip} \leq Q^{gH_2}_{i} \quad \forall i \in I, p \in P \tag{30}$$

$$q^{bgH_2}_{ip} \leq Q^{bgH_2}_{i} \quad \forall i \in I, p \in P \tag{31}$$

$$q^{eH_2}_{ip} \leq Q^{eH_2}_{i} \quad \forall z \in Z, i \in I, p \in P \tag{32}$$

$$q^{gH_2}_{ip}, q^{eH_2}_{ip}, q^{bgH_2}_{ip} \geq 0 \quad \forall z \in Z, p \in P, i \in I \tag{33}$$

Equations 34–40 present constraints for the hydrogen transport.

$$flow^{H_2}_{ii'p} \leq TG^{H_2}_{ii'} \quad \forall i \in I, i' \in JHG(i), p \in P \tag{34}$$

$$x^{in}_{ip} = \sum_{i' \in JHL(i)} tl^{H_2}_{i'ip} \quad \forall i \in I, p \in P \tag{35}$$

$$x^{in}_{ip} \leq TLG^{in}_{i} \quad \forall i \in I, p \in P \tag{36}$$

$$x^{out}_{ip} = \sum_{i' \in JHL(i)} tl^{H_2}_{ii'p} \quad \forall i \in I, p \in P \tag{37}$$

$$x^{out}_{ip} \leq TLG^{out}_{i} \quad \forall i \in I, p \in P \tag{38}$$

$$flow^{H_2}_{ii'p} \geq 0 \quad \forall i \in I, i' \in JHG(i), p \in P \tag{39}$$

$$tl^{H_2}_{ii'p} \geq 0 i \in I, i' \in JHL(i), p \in P \tag{40}$$

Equations 41–45 provide constraints for the operation of hydrogen storage.

$$inj^{H_2}_{ifp} \leq SIR^{H_2}_{if} \quad \forall i \in I, f \in F, p \in P \tag{41}$$

$$e^{H_2}_{ifp} \leq SER^{H_2}_{if} \forall i \in I, f \in F, p \in P \tag{42}$$

$$\sum_{p \in P} e^{H_2}_{ifp} \leq SC^{H_2}_{if} \quad \forall i \in I, f \in F \tag{43}$$

$$\sum_{\mathrm{p} \in P} \mathrm{e}^{\mathrm{H}_2}_{\mathrm{ifp}} \leq \sum_{\mathrm{p} \in P} \mathrm{inj}^{H_2}_{ifp} \quad \forall i \in I, f \in F \tag{44}$$

$$e^{H_2}_{ifp}, inj^{H_2}_{ifp} \geq 0 \quad \forall i \in I, f \in F, p \in P \tag{45}$$

Equations 46–49 present capacity constraints for the methane production.

$$q^{g}_{zip} \leq Q^{g}_{zi} \quad \forall z \in Z, i \in I, p \in P \tag{46}$$

$$q^{gg}_{ip} \leq Q^{gg}_{i} \quad \forall i \in I, p \in P \tag{47}$$

$$q^{H2g}_{ip} \leq Q^{H2g}_{i} \quad \forall i \in I, p \in P \tag{48}$$

$$q^{g}_{zip}, q^{gg}_{ip}, q^{H2g}_{ip} \geq 0 \quad \forall p \in P, i \in I \tag{49}$$

Equations 50–56 present the constraints for methane transport.

$$flow^{g}_{ii'p} \leq TG^{g}_{ii'} \quad \forall i \in I, i' \in JMG(i), p \in P \tag{50}$$

$$x^{gin}_{ip} = \sum_{i' \in JML(i)} tl^{g}_{i'ip} \quad \forall i \in I, p \in P \tag{51}$$

$$x^{gin}_{ip} \leq TLG^{gin}_{i} \forall i \in I, i' \in JML(i), p \in P \tag{52}$$

$$x^{gout}_{ip} = \sum_{i' \in JML(i)} tl^{g}_{ii'p} \quad \forall i \in I, p \in P \tag{53}$$

$$x^{gout}_{ip} \leq TLG^{gout}_{i} \quad \forall i \in I, p \in P \tag{54}$$

$$flow^{g}_{ii'p} \geq 0 \quad \forall i \in I, i' \in JG(i), p \in P \tag{55}$$

$$tl^{g}_{ii'p} \geq 0 \quad i \in I, i' \in JL(i), p \in P \tag{56}$$

Eqs. (57)–(61) provide constraints for the operation of methane storage.

$$inj^{g}_{inp} \leq SIR^{g}_{in} \quad \forall i \in I, n \in N, p \in P \tag{57}$$

$$e^{g}_{inp} \leq SER^{g}_{in} \quad \forall i \in I, n \in N, p \in P \tag{58}$$

$$e^{g}_{inp} \leq SC^{g}_{in} \quad \forall i \in I, n \in N \tag{59}$$

$$\sum_{p \in P} e^{g}_{inp} \leq \sum_{p \in P} inj^{g}_{inp} \quad \forall i \in I, n \in N \tag{60}$$

$$e^{g}_{inp}, inj^{g}_{inp} \geq 0 \quad \forall i \in I, f \in F, p \in P \tag{61}$$

References

[1] Arabzadeh V, Mikkola J, Jasiūnas J, Lund PD. Deep decarbonization of urban energy systems through renewable energy and sector-coupling flexibility strategies. J Environ Manage 2020;260:110090. https://doi.org/10.1016/j.jenvman.2020.110090.

[2] Riechmann C, Bothe D, Galano C, Balachandar V, Steinfort T, Kampman B, et al. Potentials of sector coupling for decarbonisation: assessing regulatory barriers in linking the gas and electricity sectors in the EU : final report; 2019.

[3] Robinius M, Otto A, Heuser P, Welder L, Syranidis K, Ryberg D, et al. Linking the power and transport sectors—Part 1: the principle of sector coupling. Energies 2017;10:956. https://doi.org/10.3390/en10070956.

[4] Gonzalez-Venegas F, Petit M, Perez Y. Electric Vehicles as flexibility providers for distribution systems. A techno-economic review. 2019. https://doi.org/10.34890/554.

[5] Cansino J, Sánchez-Braza A, Sanz-Díaz T. Policy instruments to promote electromobility in the EU28: a comprehensive review. Sustainability 2018;10:2507. https://doi.org/10.3390/su10072507.

[6] Fischer D, Wolf T, Wapler J, Hollinger R, Madani H. Model-based flexibility assessment of a residential heat pump pool. Energy 2017;118:853–64. https://doi.org/10.1016/j.energy.2016.10.111.

[7] Mollenhauer E, Christidis A, Tsatsaronis G. Increasing the flexibility of combined heat and power plants with heat pumps and thermal energy storage. J Energy Res Technol 2018;140:020907. https://doi.org/10.1115/1.4038461.

[8] Buttler A, Spliethoff H. Current status of water electrolysis for energy storage, grid balancing and sector coupling via power-to-gas and power-to-liquids: a review. Renew Sustain Energy Rev 2018;82:2440–54. https://doi.org/10.1016/j.rser.2017.09.003.

[9] Götz M, Lefebvre J, Mörs F, McDaniel Koch A, Graf F, Bajohr S, et al. Renewable power-to-gas: a technological and economic review. Renew Energy 2016;85:1371–90. https://doi.org/10.1016/j.renene.2015.07.066.

[10] Sijm J, Gockel P, van Hout M, Ozdemir O, van Stralen J, Smekens K, et al. Demand and supply of flexibility in the power system of the Netherlands, 2015–2050: Summary report of the FLEXNET project. Amsterdam: The Netherlands; 2017.

[11] Junker RG, Azar AG, Lopes RA, Lindberg KB, Reynders G, Relan R, et al. Characterizing the energy flexibility of buildings and districts. Appl Energy 2018;225:175–82. https://doi.org/10.1016/j.apenergy.2018.05.037.

[12] Conti I. Sector coupling and sector integration 2018. https://fsr.eui.eu/sector-coupling-and-sector-integration/ (accessed July 24, 2020).

[13] IO2050. Infrastructure outlook 2050: A joint study by Gasunie and TenneT on integrated energy infrastructure in the Netherlands and Germany. The Netherlands; 2019.

[14] Mancarella P, Andersson G, Pecas-Lopes JA, Bell KRW. Modelling of integrated multi-energy systems: Drivers, requirements, and opportunities. 2016 Power Systems Computation Conference (PSCC), Genoa, Italy: IEEE; 2016, p. 1–22. https://doi.org/10.1109/PSCC.2016.7541031.

[15] Riepin I, Mobius T, Musgens F. In: Integrated Electricity and Gas Market Modeling - Effects of Gas Demand Uncertainty. Lodz: IEEE; 2018. p. 1–5. https://doi.org/10.1109/EEM.2018.8469790.

[16] Özdemir Ö, van Hout M, de Joode J. Short-term price and volume interactions in an integrated gas and electricity market framework. Petten: ECN 2015.

[17] Ordoudis C, Pinson P, Morales JM. An integrated market for electricity and natural gas systems with stochastic power producers. Eur J Oper Res 2019;272:642–54. https://doi.org/10.1016/j.ejor.2018.06.036.

[18] Abeysekera M, Wu J, Nick J. Integrated energy systems: An overview of benefits, analysis methods, research gaps and opportunites. Hubnet 2016.

[19] Pambour KA. Modelling, simulation and analysis of security of supply scenarios in integrated gas and electricity transmission networks. University of Groningen 2018.

[20] Juanwei C, Tao Y, Yue X, Xiaohua C, Bo Y, Baomin Z. Fast analytical method for reliability evaluation of electricity-gas integrated energy system considering dispatch strategies. Appl Energy 2019;242:260–72. https://doi.org/10.1016/j.apenergy.2019.03.106.

[21] Tsupari E, Kärki J, Vakkilainen E. Economic feasibility of power-to-gas integrated with biomass fired CHP plant. J Storage Mater 2016;5:62–9. https://doi.org/10.1016/j.est.2015.11.010.

[22] Farahani SS, Bleeker C, van Wijk A, Lukszo Z. Hydrogen-based integrated energy and mobility system for a real-life office environment. Appl Energy 2020;264:114695. https://doi.org/10.1016/j.apenergy.2020.114695.

[23] David M, Ocampo-Martínez C, Sánchez-Peña R. Advances in alkaline water electrolyzers: a review. J Storage Mater 2019;23:392–403. https://doi.org/10.1016/j.est.2019.03.001.

[24] Cinti G, Baldinelli A, Di Michele A, Desideri U. Integration of solid oxide electrolyzer and Fischer-Tropsch: a sustainable pathway for synthetic fuel. Appl Energy 2016;162:308–20. https://doi.org/10.1016/j.apenergy.2015.10.053.

[25] Wang L, Pérez-Fortes M, Madi H, Diethelm S, herle JV, Maréchal F. Optimal design of solid-oxide electrolyzer based power-to-methane systems: A comprehensive comparison between steam electrolysis and co-electrolysis. Applied Energy 2018;211:1060–79. https://doi.org/10.1016/j.apenergy.2017.11.050.

[26] Wang L, Chen M, Küngas R, Lin T-E, Diethelm S, Maréchal F, et al. Power-to-fuels via solid-oxide electrolyzer: Operating window and techno-economics. Renew Sustain Energy Rev 2019;110:174–87. https://doi.org/10.1016/j.rser.2019.04.071.

[27] Schmidt O, Gambhir A, Staffell I, Hawkes A, Nelson J, Few S. Future cost and performance of water electrolysis: an expert elicitation study. Int J Hydrogen Energy 2017;42:30470–92. https://doi.org/10.1016/j.ijhydene.2017.10.045.
[28] Adelung S, Kurkela E, Habermeyer F, Kurkela M. Review of electrolysis technologies and their integration alternatives. VTT 2018.
[29] Store&Go. Roadmap for large-scale storage based PtG conversion in the EU up to 2050. 2019.
[30] Mondal KC, Ramesh Chandran S. Evaluation of the economic impact of hydrogen production by methane decomposition with steam reforming of methane process. Int J Hydrogen Energy 2014;39:9670–4. https://doi.org/10.1016/j.ijhydene.2014.04.087.
[31] Montenegro Camacho YS, Bensaid S, Piras G, Antonini M, Fino D. Techno-economic analysis of green hydrogen production from biogas autothermal reforming. Clean Techn Environ Policy 2017;19:1437–47. https://doi.org/10.1007/s10098-017-1341-1.
[32] Cloete S, Khan MN, Amini S. Economic assessment of membrane-assisted autothermal reforming for cost effective hydrogen production with CO2 capture. Int J Hydrogen Energy 2019;44:3492–510. https://doi.org/10.1016/j.ijhydene.2018.12.110.
[33] Ghaib K, Nitz K, Ben-Fares F-Z. Chemical methanation of CO22: a review. ChemBioEng Rev 2016;3:266–75. https://doi.org/10.1002/cben.201600022.
[34] Lecker B, Illi L, Lemmer A, Oechsner H. Biological hydrogen methanation – a review. Bioresour Technol 2017;245:1220–8. https://doi.org/10.1016/j.biortech.2017.08.176.
[35] Thema M, Bauer F, Sterner M. Power-to-gas: electrolysis and methanation status review. Renew Sustain Energy Rev 2019;112:775–87. https://doi.org/10.1016/j.rser.2019.06.030.
[36] Ditaranto M, Heggset T, Berstad D. Concept of hydrogen fired gas turbine cycle with exhaust gas recirculation: assessment of process performance. Energy 2020;192:116646. https://doi.org/10.1016/j.energy.2019.116646.
[37] Cappelletti A, Martelli F. Investigation of a pure hydrogen fueled gas turbine burner. Int J Hydrogen Energy 2017;42:10513–23. https://doi.org/10.1016/j.ijhydene.2017.02.104.
[38] Rajabi M, Mehrpooya M, Haibo Z, Huang Z. Chemical looping technology in CHP (combined heat and power) and CCHP (combined cooling heating and power) systems: a critical review. Appl Energy 2019;253:113544. https://doi.org/10.1016/j.apenergy.2019.113544.
[39] Udeh GT, Udeh PO. Comparative thermo-economic analysis of multi-fuel fired gas turbine power plant. Renewable Energy 2019;133:295–306. https://doi.org/10.1016/j.renene.2018.10.036.
[40] Liu Z, Karimi IA. New operating strategy for a combined cycle gas turbine power plant. Energy Convers Manage 2018;171:1675–84. https://doi.org/10.1016/j.enconman.2018.06.110.
[41] Luo X, Wang J, Dooner M, Clarke J. Overview of current development in electrical energy storage technologies and the application potential in power system operation. Appl Energy 2015;137:511–36. https://doi.org/10.1016/j.apenergy.2014.09.081.
[42] Zerrahn A, Schill W-P, Kemfert C. On the economics of electrical storage for variable renewable energy sources. European Economic Review 2018;108:259–79. https://doi.org/10.1016/j.euroecorev.2018.07.004.
[43] Kittner N, Lill F, Kammen DM. Energy storage deployment and innovation for the clean energy transition. Nat Energy 2017;2:17125. https://doi.org/10.1038/nenergy.2017.125.
[44] Caglayan DG, Weber N, Heinrichs HU, Linßen J, Robinius M, Kukla PA, et al. Technical potential of salt caverns for hydrogen storage in Europe. Int J Hydrogen Energy 2020;45:6793–805. https://doi.org/10.1016/j.ijhydene.2019.12.161.
[45] Michalski J, Bünger U, Crotogino F, Donadei S, Schneider G-S, Pregger T, et al. Hydrogen generation by electrolysis and storage in salt caverns: potentials, economics and systems aspects with regard to the German energy transition. Int J Hydrogen Energy 2017;42:13427–43. https://doi.org/10.1016/j.ijhydene.2017.02.102.
[46] Tarkowski R. Underground hydrogen storage: Characteristics and prospects. Renew Sustain Energy Rev 2019;105:86–94. https://doi.org/10.1016/j.rser.2019.01.051.
[47] Thompson M, Davison M, Rasmussen H. Natural gas storage valuation and optimization: a real options application: natural gas storage valuation and optimization. Nav Res Logist 2009;56:226–38. https://doi.org/10.1002/nav.20327.
[48] Blanco H, Nijs W, Ruf J, Faaij A. Potential for hydrogen and power-to-liquid in a low-carbon EU energy system using cost optimization. Appl Energy 2018;232:617–39. https://doi.org/10.1016/j.apenergy.2018.09.216.
[49] Brown T, Schlachtberger D, Kies A, Schramm S, Greiner M. Synergies of sector coupling and transmission reinforcement in a cost-optimised, highly renewable European energy system. Energy 2018;160:720–39. https://doi.org/10.1016/j.energy.2018.06.222.
[50] Robinius M, Otto A, Syranidis K, Ryberg DS, Heuser P, Welder L, et al. Linking the power and transport sectors—Part 2: Modelling a Sector coupling scenario for Germany. Energies 2017;10:957. https://doi.org/10.3390/en10070957.
[51] Maruf MdNI. Sector coupling in the North Sea Region—a review on the energy system modelling perspective. Energies 2019;12:4298. https://doi.org/10.3390/en12224298.
[52] Eriksson ELV, Gray EMacA. Optimization and integration of hybrid renewable energy hydrogen fuel cell energy systems – A critical review. Applied Energy 2017;202:348–64. https://doi.org/10.1016/j.apenergy.2017.03.132.
[53] Yan X, Zhang X, Gu C, Li F. Power to gas: addressing renewable curtailment by converting to hydrogen. Front Energy 2018;12:560–8. https://doi.org/10.1007/s11708-018-0588-5.
[54] Uyar TS, Beşikci D. Integration of hydrogen energy systems into renewable energy systems for better design of 100% renewable energy communities. Int J Hydrogen Energy 2017;42:2453–6. https://doi.org/10.1016/j.ijhydene.2016.09.086.
[55] Kaiwen L, Bin Y, Tao Z. Economic analysis of hydrogen production from steam reforming process: a literature review. Energy Sources Part B 2018;13:109–15. https://doi.org/10.1080/15567249.2017.1387619.
[56] Glenk G, Reichelstein S. Economics of converting renewable power to hydrogen. Nat Energy 2019;4:216–22. https://doi.org/10.1038/s41560-019-0326-1.
[57] Welder L, Ryberg DS, Kotzur L, Grube T, Robinius M, Stolten D. Spatio-temporal optimization of a future energy system for power-to-hydrogen applications in Germany. Energy 2018;158:1130–49. https://doi.org/10.1016/j.energy.2018.05.059.
[58] Qadrdan M, Abeysekera M, Chaudry M, Wu J, Jenkins N. Role of power-to-gas in an integrated gas and electricity system in Great Britain. Int J Hydrogen Energy 2015;40:5763–75. https://doi.org/10.1016/j.ijhydene.2015.03.004.
[59] Qadrdan M, Chaudry M, Wu J, Jenkins N, Ekanayake J. Impact of a large penetration of wind generation on the GB gas network. Energy Policy 2010;38:5684–95. https://doi.org/10.1016/j.enpol.2010.05.016.
[60] Abrell J, Gerbaulet C, Holz F, Lorenz C, Weigt H. Combining Energy Networks: The Impact of Europe's Natural Gas Network on Electricity Markets until 2050. Berlin: DIW German Institute for Economic Research; 2013.
[61] Blanco H, Nijs W, Ruf J, Faaij A. Potential of Power-to-Methane in the EU energy transition to a low carbon system using cost optimization. Appl Energy 2018;232:323–40. https://doi.org/10.1016/j.apenergy.2018.08.027.
[62] Guilera J, Ramon Morante J, Andreu T. Economic viability of SNG production from power and CO2. Energy Convers Manage 2018;162:218–24. https://doi.org/10.1016/j.enconman.2018.02.037.
[63] Ghaib K, Ben-Fares F-Z. Power-to-Methane: a state-of-the-art review. Renew Sustain Energy Rev 2018;81:433–46. https://doi.org/10.1016/j.rser.2017.08.004.
[64] Mi J, Khodayar ME. Operation of natural gas and electricity networks with line pack. J Mod Power Syst Clean Energy 2019;7:1056–70. https://doi.org/10.1007/s40565-019-0547-0.
[65] Craig M, Guerra OJ, Brancucci C, Pambour KA, Hodge B-M. Valuing intra-day coordination of electric power and natural gas system operations. Energy Policy 2020;141:111470. https://doi.org/10.1016/j.enpol.2020.111470.
[66] Chaudry M, Jenkins N, Qadrdan M, Wu J. Combined gas and electricity network expansion planning. Appl Energy 2014;113:1171–87. https://doi.org/10.1016/j.apenergy.2013.08.071.
[67] Qadrdan M, Cheng M, Wu J, Jenkins N. Benefits of demand-side response in combined gas and electricity networks. Appl Energy 2017;192:360–9. https://doi.org/10.1016/j.apenergy.2016.10.047.
[68] Ameli H, Qadrdan M, Strbac G. Coordinated operation of gas and electricity systems for flexibility study. Front Energy Res 2020;8:120. https://doi.org/10.3389/fenrg.2020.00120.
[69] CEDelft. Grid for the Future. CE Delft; 2017.
[70] Yuan H, Li F, Wei Y, Zhu J. Novel linearized power flow and linearized OPF models for active distribution networks with application in distribution LMP. IEEE Trans Smart Grid 2018;9:438–48. https://doi.org/10.1109/TSG.2016.2594814.
[71] Yang Z, Xie K, Yu J, Zhong H, Zhang N, Xia QX. A general formulation of linear power flow models: basic theory and error analysis. IEEE Trans Power Syst 2019;34:1315–24. https://doi.org/10.1109/TPWRS.2018.2871182.
[72] Metzler C, hobbs B, Pang J-S. Nash-Cournot Equilibria in Power Markets on a Linearized DC Network with Arbitrage: Formulations and Properties. Networks and Spatial Economics 2003;3:123–50. https://doi.org/10.1023/A:1023907818360.
[73] Midthun KT. Optimization models for liberalized natural gas markets. NTNU 2007.
[74] Gabriel SA, Conejo AJ, Fuller JD, Hobbs BF, Ruiz C. Complementarity Modeling in Energy Markets. vol. 180. New York, NY: Springer New York; 2013. https://doi.org/10.1007/978-1-4419-6123-5.
[75] Gabriel SA, Conejo AJ, Fuller JD, Hobbs BF, Ruiz C. Natural Gas Market Modeling. Complementarity Modeling in Energy Markets, vol. 180, New York, NY: Springer New York; 2013, p. 433–76. https://doi.org/10.1007/978-1-4419-6123-5_10.
[76] Tejada-Arango DA, Domeshek M, Wogrin S, Centeno E. Enhanced representative days and system states modeling for energy storage investment analysis. IEEE Trans Power Syst 2018;33:6534–44. https://doi.org/10.1109/TPWRS.2018.2819578.
[77] AIMMS. AIMMS 2020. https://www.aimms.com/ (accessed June 19, 2020).
[78] IBM. CPLEX. IBM; 2019.
[79] ESDL. ESDL MAPEDITOR. The Hague: TNO; 2020.
[80] CA. Climate Agreement 2019.
[81] den Ouden B, Kerkhoven J, Warnaars J, Terwel R, Coenen M, Verboon T, et al. Climate neutral energy scenarios 2050. The Netherlands: Barenschot/Kalavasta; 2020.
[82] UNFCCC. The Paris Agreement. United Nations Climate Change 2016. https://unfccc.int/process-and-meetings/the-paris-agreement/the-paris-agreement (accessed June 16, 2020).
[83] ETM. Energy Transition Model 2020. https://energytransitionmodel.com/ (accessed June 30, 2020).